1994

The Synthesis and Characterization of RuII(bpy){(bpyrm)RuII(NH3)4}2](PF6)6 and [RuII(bpy)2(bpyrm)RuII(NH3)4](PF6)4

Rick Anthony Pavinato

THESIS REPRODUCTION CERTIFICATE

TO: Graduate Degree Candidates who have written formal theses.

SUBJECT: Permission to reproduce theses.

The University Library is receiving a number of requests from other institutions asking permission to reproduce dissertations for inclusion in their library holdings. Although no copyright laws are involved, we feel that professional courtesy demands that permission be obtained from the author before we allow theses to be copied.

Please sign one of the following statements:

Booth Library of Eastern Illinois University has my permission to lend my thesis to a reputable college or university for the purpose of copying it for inclusion in that institution's library or research holdings.

_____ / _____ / _____

Date Author

I respectfully request Booth Library of Eastern Illinois University not allow my thesis be reproduced because _____

_____

_____

_____ _____

Date Author

m

The Synthesis and Characterization of

$[Ru^{II}(bpy)\{(bpyrm)Ru^{II}(NH_3)_4\}_2](PF_6)_6$ and $[Ru^{II}(bpy)_2(bpyrm)Ru^{II}(NH_3)_4](PF_6)_4$

(TITLE)

BY

Rick Anthony Pavinato

THESIS

SUBMITTED IN PARTIAL FULFILLMENT OF THE REQUIREMENTS
FOR THE DEGREE OF

Master of Science in Chemistry

IN THE GRADUATE SCHOOL, EASTERN ILLINOIS UNIVERSITY
CHARLESTON, ILLINOIS

1994

YEAR

I HEREBY RECOMMEND THIS THESIS BE ACCEPTED AS FULFILLING
THIS PART OF THE GRADUATE DEGREE CITED ABOVE

5-6-94
DATE

ADVISER

5/6/94
DATE

DEPARTMENT HEAD

The Synthesis and Characterization of $[Ru^{II}(bpy)\{(bpyrm)Ru^{II}(NH_3)_4\}_2](PF_6)_6$ and $[Ru^{II}(bpy)_2(bpyrm)Ru^{II}(NH_3)_4](PF_6)_4$

Thesis Approved By :

Dr. Ellen Keiter Date

Dr. Robert Karraker Date

Dr. David Buchanan Date

Dr. Mark McGuire Date

We do not ask for what useful purpose the birds do sing, for song is their pleasure since they were created for singing. Similarly, we ought not to ask why the human mind troubles to fathom the secrets of the heavens.....
The diversity of the phenomena of Nature is so great, and the treasures hidden in the heavens so rich, precisely in order that the human mind shall never be lacking in fresh nourishment.

- Johannes Kepler, *Mysterium Cosmographicum*

I wish to thank my beautiful wife Cindy, and my family (Mom, Dad, and Gram) for all their support. Also, I would like to thank Ken and Matt - who always had just what I needed. Last, but never least, I would like to thank Dr. Mark McGuire - I could never begin to repay his time and effort put forth on this project - You have my deepest respect and gratitude. Once again, Thank you all.

Abstract

This thesis describes the synthesis of a trimetallic Ru^{II} complex $[Ru^{II}(bpy)\{(bpyrm)Ru^{II}(NH_3)_4\}_2](PF_6)_6$ and its bimetallic analog $[Ru^{II}(bpy)_2(bpyrm)Ru^{II}(NH_3)_4](PF_6)_4$. The trimetallic species was designed to be the first in a series of complexes where the reduction potential of the "bridging" complex could be varied (relative to the "terminal" sites) through systematic variation in the metal (M) and/or ligand (LL) :

$$[(NH_3)_4Ru^{II}\text{-bpyrm-}M^{II}(LL)\text{-bpyrm-}Ru^{II}(NH_3)_4]^{6+}$$

where : M = Ru or Os

LL = 2,2'-bipyridine (bpy), 1,10-phenanthroline, and derivatives.

bpyrm = 2,2'-bipyrimidine.

Generation of the $[Ru^{II}\text{-}M^{II}\text{-}Ru^{III}]$ "mixed-valence" complex would then allow observation of "end-to-end" intervalence charge transfer (IVCT) as a function of bridge potential.

The initial bi- and trimetallic complexes were synthesized and characterized. In addition, the [2,3] and [3,2,3] "mixed-valence" forms of these complexes were generated and studied. However, a persistent impurity, originating from a side reaction of one of the starting materials, made it difficult to generate the target [2,2,3] mixed-valence form of the trimetallic species. Rigorous attempts to purify the complexes are described in detail.

Table of Contents

Table of Contents

Table of Contents

List of Tables

List of Figures

List of Figures

List of Figures

Introduction

Electron transfer reactions (ET) are fairly common in various inorganic, organic, and biological systems. For example, in photosynthesis a series of efficient light-induced ET reactions are used by green plants to produce high energy products. Recently, attempts to model these systems have involved redox-active transition metal complexes. In developing complexes that can be studied there are many properties that limit system selection. Ideally a system should contain: 1) two or more substitutionally inert metal complexes; 2) bridging ligands which connect the metal centers and serve as routes for intramolecular ET ; 3) metal centers that are readily oxidized or reduced; and 4) intermediates and/or products that are substitutionally inert.

In the past 30 years, there has been a vast amount of theoretical and experimental work done in the area of long distance ET. This has led to a greatly increased understanding of how the efficiency of the process varies with distance, temperature, free energy (ΔG), solvent properties, and molecular orientations. This study deals exclusively with attempts to synthesize and monitor intramolecular ET in "mixed-valence" M(II) - M(III) bridged complexes based on the d^6-d^5 metal centers of ruthenium. Insights gained by studying long distance ET reactions in these model systems may contribute to an increased understanding of other systems (photosynthesis) and to the design of increasingly efficient chemical solar energy conversion schemes.

A typical mixed-valence species, such as :

$$M_a^{II} \sim\sim\sim M_b^{III}$$

can be produced by one electron oxidation of the M_a^{II} ~~~ M_b^{II} precursor. The two neighboring metal ions M_a^{II} and M_b^{III} are each surrounded by a coordination environment which may consist of similar or different numbers and types of ligands, and are connected by a common ligand or bridge (~~~).[1] M_a^{II} and M_b^{III} can be the same or different type of metal. As illustrated here, they usually differ by one unit in their oxidation states. The bridging group may be an aromatic heterocycle, an organic chain, a single atom, a metal-metal bond, or even a protein. The type of bridge greatly affects the efficiency of intramolecular ET between the metal centers in the complex.

A mixed-valence, bimetallic species where the metal centers are identical (except, of course, for their oxidation state) can be represented as :

$$M^{II}\sim\sim\sim M^{III}$$

Several important questions can be raised concerning this species.

1) What is the rate of interconversion to the "redox isomer"?

$$M^{II}\sim\sim\sim M^{III} \quad <\text{-------}> \quad M^{III}\sim\sim\sim M^{II}$$

(In other words, what is the rate constant, k_{ET},(s^{-1}), of thermal intramolecular ET from M^{II} --> M^{III}).

2) What is the activation energy, E_a, for this interconversion?

3) How do the electronic characteristics of the bridge (~~~) between M^{II} and M^{III} affect the efficiency of intramolecular thermal ET?

According to Robin and Day[2], mixed-valence systems can be divided into three different types or classes. Class I compounds show little or no electronic interaction between the metal centers (because the $M^{II}\sim\sim\sim M^{III}$ separation is large or because their immediate environments are very different). Class II compounds show a weak amount of interaction, and in Class III compounds the electronic interaction between the two metal centers is so great that the individual characteristics of each metal are nonexistent (the "odd" electron is considered to be delocalized). The compounds in this thesis were designed to show Class II (weak interaction) behavior.

An intramolecular electron transfer reaction in a symmetric mixed-valence $M^{II}\sim\sim\sim M^{III}$ complex can be represented by the potential energy diagram in Figure 1-1. The reactant ($M^{II}\sim\sim\sim M^{III}$) and product ($M^{III}\sim\sim\sim M^{II}$) states are depicted by one-dimensional slices of three-dimensional potential energy surfaces representing the nuclear positions and energies (including solvent) before and after ET takes place (Figure 1-1 is admittedly an oversimplification of the overall ET event. However, such representations are regularly used in the literature and are valuable for demonstrating the important parameters involved in the process.)

In a Class II mixed-valence species, the small amount of electronic interaction does cause a finite "splitting" at the crossing point of the two potential surfaces. In Figure 1-1, this splitting is represented by $2H_{ab}$. (The magnitude of H_{ab} is considered to be a measure of the "electronic communication" between the metal centers.) Electron transfer occurs at the intersection of the two curves because energy must be conserved and it is only at this point that the energies are the same immediately before and after ET. The electron transfer event ("thermal" ET) can be described (using Figure 1-1) as a passage of the system from the ($M^{II}\sim\sim\sim M^{III}$) state to the ($M^{III}\sim\sim\sim M^{II}$) state.

Despite the fact that the overall free-energy change for the process is zero, an activation barrier (energy = E_a) does exist. This activation energy arises from both solvent (repolarization; E_{out}) and intramolecular (metal-ligand bond length changes; E_{in}) reorganization energies resulting from charge transfer. Thus, the total reorganization energy, $E_r = E_{in} + E_{out} = E_a$. Additionally,

$$E_{in} = n\,[(2\,f_2\,f_3)/f_2 + f_3]\,(d_2 - d_3)^2 \qquad (1)$$

$$E_{out} = e^2\,(1/2a_2 + 1/2a_3 - 1/r)\,(1/D_{op} - 1/D_s) \qquad (2)$$

E_{in} is the inner-sphere reorganization energy (due to metal-ligand bond length adjustments), where n is the number of ligands per metal center, and f_2, f_3 and d_2, d_3 are the force constants and equilibrium bond lengths, respectively, for the metal-ligand bonds for $\mathbf{M^{II}}$ and $\mathbf{M^{III}}$. E_{out} is the outer-sphere (or solvent) reorganization energy, where e is the electronic charge, a_2 and a_3 are the "effective radii" of the $\mathbf{M^{II}}$ and $\mathbf{M^{III}}$ complexes, r is the separation between the metal centers, and D_{op} and D_s are the optical and static dielectric constants of the solvent. Thus ET would be slow (high E_a) in a system where large metal-ligand bond length changes occurred and/or where E_{out} was large (usually due to a high D_s value : eg, polar solvents).

A second ET pathway is shown in Figure 1-1. Electron transfer can occur through optical excitation of the $\mathbf{M^{II}{\sim}{\sim}{\sim}M^{III}}$ species to a vibrationally excited $[\mathbf{M^{III}{\sim}{\sim}{\sim}M^{II}}]^*$ state. This optical transition, of energy E_{op}, appears as a vertical transition in Figure 1-1. This is called a metal to metal charge transfer (MMCT) or intervalence charge transfer (IVCT) transition. Hush[3] has shown that, for a symmetric weakly coupled Class II mixed-valence complex :

$$E_a = E_{op}/4 = E_r/4 \qquad (3)$$

Figure 1-1 : Potential Energy versus Nuclear Configuration for a Symmetric Mixed-Valence Complex.

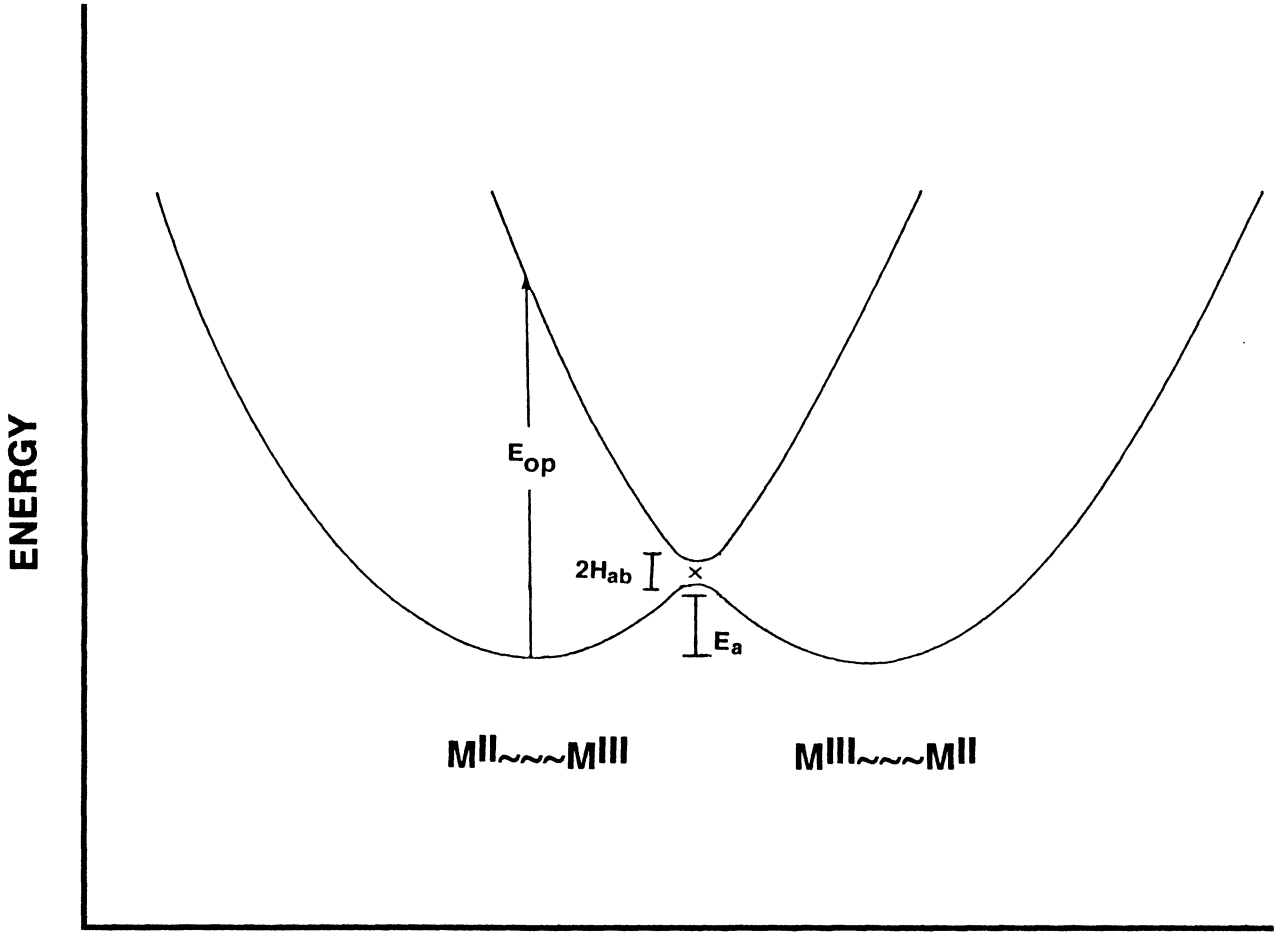

where E_r is the total reorganization energy and E_a is the activation barrier for thermal ET.

Hush's theory has also been used to relate E_{op} to H_{ab} :

$$H_{ab} = 2.05 \times 10^{-2} [\epsilon_{max} \Delta\bar{\nu}_{1/2} / E_{op}]^{1/2} (E_{op}/r) \text{ cm}^{-1} \quad (4)$$

where : $$\Delta\bar{\nu}_{1/2} = [2310 E_{op}]^{1/2} \text{ cm}^{-1} \quad . \quad (5)$$

Referring to the IVCT absorption, $\Delta\bar{\nu}_{1/2}$ is the bandwidth at half intensity and ϵ_{max} is the molar absorptivity (M^{-1} cm^{-1}) at the band maximum. It can be noted (from Eq. 3 through 5) that if E_{op} is high and ϵ_{max} is low, then E_a will be high and H_{ab} will be low , which would predict that the rate of thermal ET in Eq. 6 would be low.

$$[M^{II}\sim\sim\sim M^{III}] \quad \text{------>} \quad [M^{III}\sim\sim\sim M^{II}] \quad (6)$$

On the other hand, if E_{op} is low and ϵ_{max} is high, E_a will be low and H_{ab} will be larger (i.e. the rate of thermal ET will be high in Eq. 6).

Table 1-1 shows data obtained for two different symmetric mixed-valence bimetallic complexes. As can be observed from the data, when the distance between the metal centers increases, E_{op} increases, and both ϵ_{max} and H_{ab} decrease. This would imply a smaller rate of thermal ET would result when the distance between the metal center increases - an expected result.

When the two metal sites in a $M^{II}\sim\sim\sim M^{III}$ mixed-valence species are not equivalent ("asymmetric"), intramolecular ET occurs with a net free energy change. Figure 1-2 can be used to represent this situation. (It is common in the literature to assume that overall entropy changes for ET in these systems

Table 1-1 : Intervalence Spectra of Class II $[Ru(bpy)_2Cl]_2L\text{-}L^{3+}$ in CH_3CN.[4]

L-L	r, Å	nm	ϵ_{max}, M^{-1} cm^{-1}	$\Delta\nu_{1/2}$ cm^{-1}	H_{ab}, cm^{-1}	E_{op}, cm^{-1}
pyrazine	6.8	1300	450	5000	400	7692
4,4'-bpy	11.3	980	100	4900	150	10,204

are zero; $\Delta S \approx 0$. The overall free energy change, ΔG_o, is then approximated as ΔE_o, where ΔE_o equals the difference in the reduction potentials of the two metal sites).

It should be noted that for an asymmetric mixed-valence species (Figure 1-2) :

$$E_{op} = \Delta E_o + E_r \tag{7}$$

Additionally, it can be shown that :

$$E_a\ (3,2 \dashrightarrow 2,3) = (E_{op} - 2\Delta E_o)^2 / 4(E_{op} - \Delta E_o) \tag{8}$$

Also for the asymmetric case :

$$H_{ab} = 2.05 \times 10^{-2} \left[(\epsilon_{max}\ \Delta\bar{\nu}_{1/2}) / E_{op} \right]^{1/2}\ (E_{op}/r)\ \text{cm}^{-1} \tag{9}$$

The effect of introducing a ΔE_o term on E_{op} can be seen by comparison of the reported IVCT bands for the following complexes :

$$[(NH_3)_5Ru^{II}\text{-}(4,4'\text{-bpy})\text{-}Ru^{III}(NH_3)_5]^{5+}$$

(I)

$$[(bpy)_2ClRu^{II}\text{-}(4,4'\text{-bpy})\text{-}Ru^{III}(NH_3)_5]^{5+}$$

(II)

where bpy = 2,2'-bypridine and 4,4'-bpy = 4,4'-bpyridine. For complex I, E_{op} = 971 cm^{-1} and for complex II, E_{op} = 1441 cm^{-1}.

Figure 1-2 : Potential Energy versus Nuclear Configuration for an Asymmetric Mixed-Valence Complex.

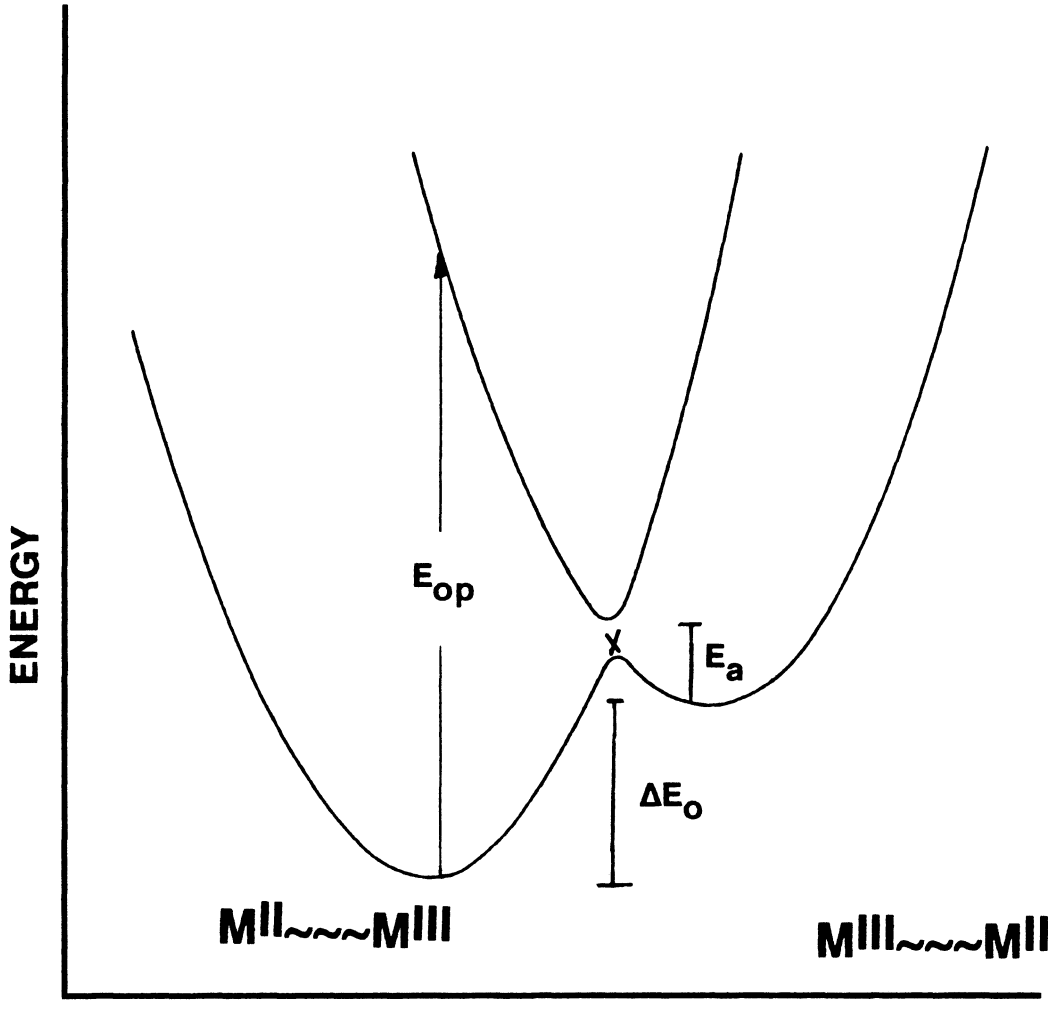

Recently, there has been an interest in examining trimetallic mixed-valence systems where the organic bridges in the bimetallic species are effectively replaced by metal complexes :

$$M^{II}\sim\sim\sim M^{II}\sim\sim\sim M^{III} \quad .$$

For example, Scandola et al.[5] have reported the synthesis of the following mixed-valence, trimetallic species :

$$[py(NH_3)_4Ru^{II}\text{-}NC\text{-}Ru^{II}(bpy)_2\text{-}CN\text{-}Ru^{III}(NH_3)_4py]^{5+} \quad .$$

(III)

where py = pyridine. It should be noted that such a complex might show two IVCT transitions arising from two separate optical ET reactions :

1. Central "$Ru^{II}(bpy)_2$" to terminal "$Ru^{III}(NH_3)_4py$"; $Ru_c^{II} \rightarrow Ru_t^{III}$ ($E_{op}[1]$)

2. Terminal "$py(NH_3)_4Ru^{II}$" to terminal "$Ru^{III}(NH_3)_4py$"; $Ru_t^{II} \rightarrow Ru_t^{III}$ ($E_{op}[2]$).

Not surprisingly, the first transition has a higher intensity (ϵ_{max}) than the second, due to the difference in distances involved,
(eg. $E_{op}[1] = 13{,}300\ cm^{-1}$ ($\epsilon_{max} = 2900\ M^{-1}cm^{-1}$) and $E_{op}[2] = 8200\ cm^{-1}$ ($\epsilon_{max} = 350\ M^{-1}cm^{-1}$)).[5]

Other trimetallic systems have also been synthesized, and these are listed in Table 1-2. Table 1-2 shows the energies and intensities of the IVCT transitions resulting from optically induced intramolecular ET between terminal Ru sites (Ru_t) in both cis and trans trimetallic complexes in the [2,2,3] oxidation

states. It can be seen from this data that the extent of electronic communication (as measured by the energy (E_{op}) and the intensity (ϵ_{max}) of the IVCT bands) is <u>not</u> a simple inverse function of "through-space" distance (r_s) between the terminal Ru sites. As an example; Meyer et al.[7] have observed no interaction between terminal Ru sites in the following complexes (r_s = ≥ 10 Å) ::

$$[(NH_3)_5Ru^{II}\text{-pz-}Ru^{II}(bpy)_2\text{-pz-}Ru^{III}(NH_3)_5]^{7+}$$

(IV)

and

$$[(NH_3)_5Ru^{II}\text{-(4,4'-bpy)-}Ru^{II}(bpy)_2\text{-(4,4'-bpy)-}Ru^{III}(NH_3)_5]^{7+}\ ;$$

(V)

where pz = pyrazine. However, Sutin et al.[6] have shown significant electron exchange in :

$$[(NH_3)_5Ru^{II}\text{-(4-CNpy)-}Ru^{II}(bpy)_2\text{-(4-CNpy)-}Ru^{III}(NH_3)_5]^{7+}$$

(VI) .

For complex VI, r_s = 13.2 Å (Table 1-2). The most dramatic comparisions can be made from the work of Taube et al.[8], for the complex :

$$\text{trans-}[(NH_3)_5Ru^{II}\text{-pz-}Ru^{II}(NH_3)_4\text{-pz-}Ru^{III}(NH_3)_5]^{7+}$$

(VII) .

Table 1-2 : IVCT Transitions for Trimetallic Complexes.

complex	λ_{max} (nm)	ϵ_{max} M^{-1} cm^{-1}	solvent	r_s, Å	ref.
$[(pz)Ru^{II}{}_4$-NC-Rx-CN-$Ru^{III}{}_5(pz)]^{5+}$					
$Ru_t \rightarrow Ru_t$	1219	350	D_2O	7.0	5
$Ru_c \rightarrow Ru_t$	752	2900			
$[(NH_3)_5Ru^{II}$-NC-Rx-CN-$Ru^{III}(NH_3)_5]^{5+}$					
$Ru_t \rightarrow Ru_t$	1053	350	D_2O	7.0	5
$Ru_c \rightarrow Ru_t$	685	3250			
$[(pz)Ru^{II}{}_4$-NC-Rx-CN-$Ru^{III}(NH_3)_5]^{5+}$					
$Ru_t \rightarrow Ru_t$	1000	370	D_2O	7.0	5
$Ru_c \rightarrow Ru_t$	680	3100			
$[Ru^{II}{}_5$-(4-CNpy)-Rx-(4-CNpy)-$Ru^{III}{}_5]^{7+}$					
$Ru_t \rightarrow Ru_t$	1090	20	CH_3CN	13.2	6
$Ru_c \rightarrow Ru_t$	625	400			
$[(NH_3)_5Ru^{II}$-pz-Rx-pz-$Ru^{III}(NH_3)_5]^{7+}$					
$Ru_t \rightarrow Ru_t$	not observed		CH_3CN	~10	7
$Ru_c \rightarrow Ru_t$	not observed				
$[Ru^{II}{}_5$-(4,4'-bpy)-Rx-(4,4'-bpy)-$Ru^{III}{}_5]^{7+}$					
$Ru_t \rightarrow Ru_t$	not observed		CH_3CN	>10	7
$Ru_c \rightarrow Ru_t$	not observed				
trans-$[Ru^{II}{}_5$-pz-$Ru^{II}(NH_3)_4$-pz-$Ru^{III}{}_5]^{7+}$					
$Ru_t \rightarrow Ru_t$	1695	~1000	D_2O	14.0	8

r_s = "though-space" distance between terminal Ru sites.

Rx = $Ru^{II}(bpy)_2$ Ru_c = central Ru 4,4'-bpy = 4,4'-bipyridine

Ru_5 = $Ru(NH_3)_5$ Ru_t = Ru of terminal $Ru(NH_3)_5^{2+/3+}$ unit

Ru_4 = $Ru(NH_3)_4$ 4-CNpy = 4-cyanopyridine

pz = pyrazine

This complex shows strong electronic interaction between the terminal sites despite having the longest end-to-end distance (14 Å).

The data presented in Table 1-2 suggests that the amount of "electronic interaction" between terminal Ru sites in trimetallic complexes is affected by other factors besides distance. Taube et al.[8] have proposed that the larger degree of end-to-end interaction in the trans complexes may be related to the more favorable "energy match" between the bridging and terminal positions. In other words, in complex (VII), the energy gap between the [2,2,3] and [2,3,2] state is not large (ie. the bridging complex is not much harder to oxidize than the terminal Ru sites). However, as seen in complexes (IV) and (V) the πd levels of the bridging "-$Ru^{II}(bpy)_2$-" are much lower in energy relative to the terminal Ru^{II} sites (ie. the bridging complex is much harder to oxidize than the terminal sites). This can be illustrated quite simply in Figure 1-3.

The synthesis and characterization of a series of trimetallic complexes where only the $\Delta E_{1/2}$ value (Figure 1-3) varies might provide a way of testing the importance of an "energy match" across the complex. The general formula of the proposed trimetallic series is :

$$[(NH_3)_4Ru^{II}\text{-bpyrm-}M^{II}(LL)\text{-bpyrm-}Ru^{II}(NH_3)_4]^{6+}$$

where : M = Ru or Os

LL = polypyridyl derivatives .

bpyrm = 2,2'-bipyrimidine

Some advantages of this series would be: 1) the ruthenium, ammine, and polypyridyl chemistry is well known; 2) the polypyridyl groups lend stability to the complex; 3) the terminal Ru sites have strong σ donating ammine ligands, preventing competition for electron density between the bridging and terminal

Figure 1-3 : Comparision of the Energy Difference in cis- versus trans-Complexes.

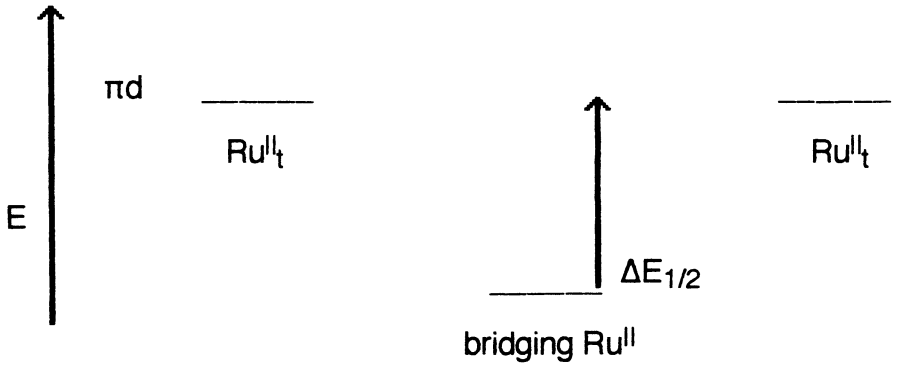

$[(NH_3)_5Ru^{II}\text{-pz-}Ru^{II}(bpy)_2\text{-pz-}Ru^{III}(NH_3)_5]^{7+}$

and

$[(NH_3)_5Ru^{II}\text{-(4,4'-bpy)-}Ru^{II}(bpy)_2\text{-(4,4'-bpy)-}Ru^{III}(NH_3)_5]^{7+}$

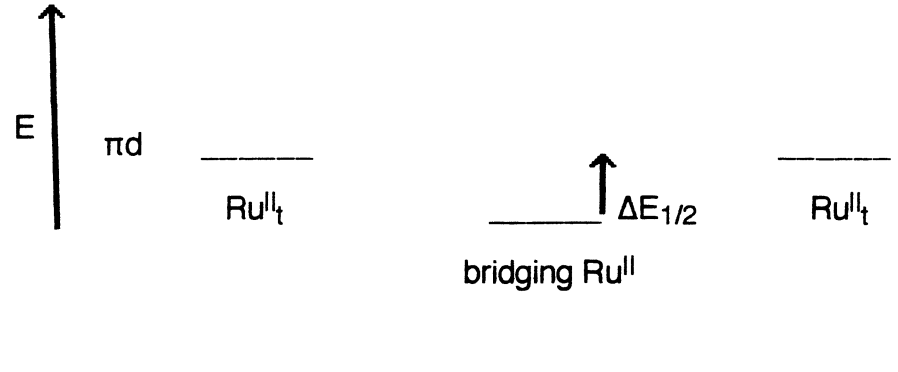

trans-$[(NH_3)_5Ru^{II}\text{-pz-}Ru^{II}(NH_3)_4\text{-pz-}Ru^{III}(NH_3)_5]^{7+}$

ligands; 4) the make-up of the trimetallic species allows for synthetic variations on the bridge (M = Ru or Os; LL = various polypyridyl ligands) allowing systematic changes of the reduction potential of the bridging metal complex relative to the terminal Ru sites, (variation of $\Delta E_{1/2}$); 5) the distance (and orientation) between the terminal Ru^{II} sites stays constant.

This thesis deals with the synthesis and characterization of the first in this series of trimetallic species (M = Ru; LL = 2,2'-bipyridine) : $[Ru^{II}(bpy)\{(bpyrm)Ru^{II}(NH_3)_4\}_2](PF_6)_6$. The structure of the [2,2,2] form is shown in Figure 1-4.

The bimetallic species, $[Ru^{II}(bpy)_2(bpyrm)Ru^{II}(NH_3)_4](PF_6)_4$, was also synthesized and characterized as an aid in understanding the electrochemical and spectroscopic characteristics of the trimetallic species. The bimetallic complex can be represented by the structure shown in Figure 1-5.

Figure 1-4 : The structure of $[Ru^{II}(bpy)\{(bpyrm)Ru^{II}(NH_3)_4\}_2]^{6+}$ in the [2,2,2] form.

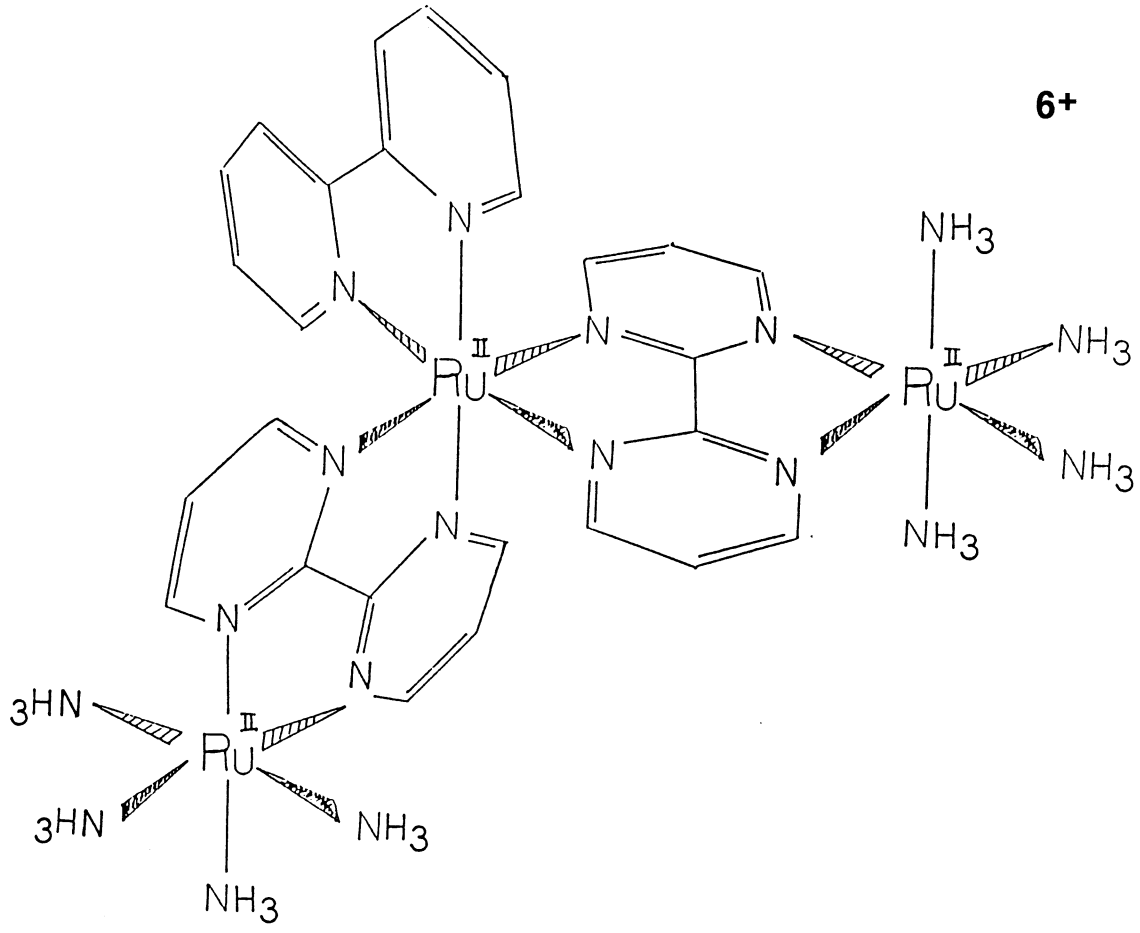

Figure 1-5 : The structure of $[Ru^{II}(bpy)_2(bpyrm)Ru^{II}(NH_3)_4]^{4+}$ in the [2,2] form .

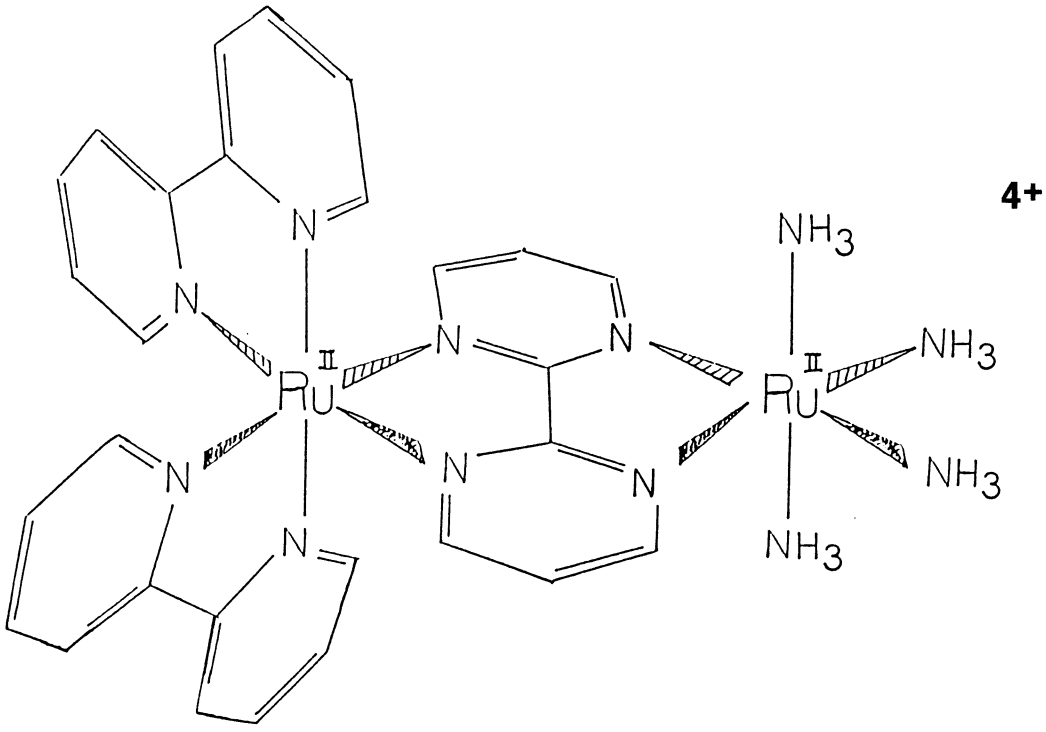

References

(1) Day, P. *Int. Rev. Phys. Chem.* **1981**, *1*, 149-193.

(2) Robin, M. B.; Day, P. *Adv. Inorg. Chem. Radiochem.* **1967**, *10*, 247.

(3) a.Allen, G. C.; Hush, N. S. *Prog. Inorg. Chem.* **1967**, *8*, 357.

b.Hush, N. S. *Prog. Inorg. Chem.* **1967**, *8*, 391.

c.Hush, N. S. *Electrochimica Acta* **1968**, *13*, 1005-1023.

(4) Creutz, C. *Prog. Inorg. Chem.*; Lippard, S. J. Ed.; John Wiley & Sons: New York, 1983; pp 1-73.

(5) a.Bignozzi, C. A.; Roffia, S.; Scandola, F. *J.Am. Chem. Soc.* **1985**, *107*, 1644-1651.

b.Bignozzi, C. A.; Paradisi, C.; Roffia, S.; Scandola, F. *Inorg. Chem.* **1988**, *27*, 408-414.

(6) Creutz, C.; Katz, N. E.; Sutin, N. *Inorg. Chem.* **1988**, *27*, 1687-1694.

(7) Powers, M. J.; Callahan, R. W.; Salmon, D. J.; Meyer, T. J. *Inorg. Chem.* **1976**, *15*, 894-900.

(8) von Kameke, A.; Tom, G. M.; Taube, H. *Inorg. Chem.* **1978**, *17*, 1790-1796.

Experimental Section

Materials. The following were purchased from Aldrich Chemical Co. and used as received : ruthenium(III) chloride hydrate ($Ru^{III}Cl_3 \cdot x\ H_2O$), 2,2'-bipyridine (bpy, 99+%), silver trifluoromethanesulfonate (AgTFMS, 99+%), trifluoromethanesulfonic acid (CF_3SO_3H, 98+%), ethylene glycol (99.5%, gold label), 2,3-dihydroxynaphthalene (H_2dhn, 98 %), potassium hexafluorophosphate (KPF_6, 98+%), acetonitrile (CH_3CN, 99.5%, ACS reagent), dimethyl sulfoxide (DMSO, 99.9%, spectrophotometric grade), tetraethylammonium chloride hydrate (TEAC, dried for five days in a vacuum oven at 80°C), white quartz sand (50-70 mesh), N,N-dimethylformamide (DMF, 99+%, spectrophotometric grade), and nitromethane (96%, spectrophotometric grade). Potassium chloride (KCl, reagent grade), neutral alumina (Al_2O_3, 80-200 mesh), DMSO (ACS certified), and disodium ethylenediaminetetraacetate (Na_2H_2EDTA, ACS certified) were purchased from Fisher Chemical Co. and used as received. Polarographic grade tetraethylammonium perchlorate (TEAP) was purchased from GFS Chemicals and used as received. Polarographic grade tetrabutylammonium hexafluorphosphate (TBAH) was purchased from BAS Chemicals and used as received. High purity Burdick & Jackson CH_3CN and propylene carbonate were purchased from Baxter Corp. and used as received. 2,2'-Bipyrimidine (bpyrm) was purchased from Lancaster Synth. Ltd. and used as received. All water used for reactions and columns was purified from a "Milli-Q™ Water System". Most organic solvents used for electrochemical experiments were stored over 3Å or 4Å "Molecular Sieves" purchased from MCB Manufacturing Chemists. Argon gas was scrubbed with a column of "Oxy-Clear" purchased from Fisher Chem. Co. (removed oxygen to a limit less than 50 ppm).

Chloropentaammine ruthenium (III) chloride ($[Ru^{III}(NH_3)_5Cl]Cl_2$) was purchased from Strem Chemicals Inc. and was recrystallized by dissolving 1.4

grams in 240 mL of 0.1M HCl at 40°C. The solution was then filtered hot and reprecipitated by addition of 2 mL of concentrated HCl. Cooling in an ice bath yielded bright yellow crystals.

Methods. Visible, ultraviolet, and near-infrared spectra were recorded on a Shimadzu UV-3100 UV-vis-NIR recording spectrophotometer. Electrochemical measurements were made using a saturated sodium chloride calomel electrode (SSCE) as a reference (room temperature) and are uncorrected for junction potential effects. A 1.5 mm platinum button electrode (for CH_3CN) or a glassy carbon electrode (for H_2O) were used as the working electrodes and a platinum wire was used as the auxiliary electrode. The electrolyte was either 0.1M TEAP or TBAH (for CH_3CN) or KCl (for H_2O). Cyclic voltammetry measurements were made with an EG&G PAR Model 173 potentiostat for potential control with a Model 175 universal programmer as a sweep generator. Voltammograms were recorded on a Houston Instruments Omnigraphic 2000 xy-recorder. The $E_{1/2}$ values from cyclic voltammetry were calculated from half the sum of the E_p (potential at current maximum) values for the anodic and cathodic waves. Elemental analyses were performed by Galbraith Laboratories Inc., Knoxville, TN, or by Atlantic Microlabs, Norcross, GA.

$Ru(bpy)Cl_4$ - The procedure of Krause[1] was followed. In a typical preparation $Ru^{III}Cl_3 \cdot 3\ H_2O$ (3.00 g, 11.5 mmol) and bpy (2.199 g, 14.1 mmol) were added to 15 mL of 1.00 N HCl. The suspension was stirred and the mixture was stoppered and left to stand 27 days in the dark. The product was collected on a medium glass frit, washed with 15 mL of cold water, and dried in vacuo. Yield : 4.04 g, 88%. (It is believed that the final product is actually

$Ru^{III}(bpy)Cl_3(H_2O)_2$, rather than $Ru(bpy)Cl_4$ as cited in the original work of Krause. In this case the yield = 92%).

cis-$Ru^{II}(bpy)_2Cl_2 \cdot 2H_2O$ - The procedure of Meyer[3] was followed with some slight modification. In a typical preparation, $Ru^{III}Cl_3 \cdot 3H_2O$ (1.95 g, 7.45 mmol), bpy (2.34 g, 15.0 mmol), and LiCl (2.10 g, 50 mmol) were heated at reflux with stirring in DMF (15 mL) for 8 hours. The reaction mixture was cooled to room temperature, 75 mL of reagent grade acetone was added and the solution was refrigerated at ~5 °C overnight. The solution was filtered in a medium porosity glass frit which yielded a red filtrate and a black precipitate. The solid was washed three times with 25 mL portions of water followed by three 25 mL portions of diethyl ether, and then dried in vacuo. Yield : 66 %, 3.88 g.

The crude product was purified by the method of Sprintschnik[4]. In a typical preparation, $Ru^{II}(bpy)_2Cl_2 \cdot 2 H_2O$ (2.5 g, 4.8 mmol) was heated at reflux with stirring in a 1:1 ethanol/water mixture for 1 hour. The insoluble solids were filtered out through a medium glass frit and LiCl (48.0 g, 1.13 mol) was added prior to rotovapping off the excess ethanol. The solution was cooled in an ice bath for 30 minutes, and the product precipitated out as very fine, dark crystals. The product was collected on a medium glass frit, washed with a small amount of cold water and dried in vacuo. Yield : 2.29 g, 90%.

$[Ru^{II}(bpy)_2(bpyrm)](PF_6)_2 \cdot H_2O$ - The procedure of Rillema[5] and coworkers was followed with some modifications. In a typical preparation $Ru^{II}(bpy)_2Cl_2 \cdot 2H_2O$ (.300 g, .576 mmol) was reacted for 45 minutes with AgTFMS (.296 g, 1.152 mmol) under a nitrogen blanket in 50 mL of reagent acetone that had previously been deaerated with N_2 for 30 minutes. The AgCl that was formed was filtered through a medium glass frit. Bpyrm (.2733 g, 1.728

mmol) was added to the maroon filtrate and the solution was heated at reflux under nitrogen for 24 hours. The appearance of a fine yellow-brown solid was noted throughout the reaction. The solution was allowed to cool to room temperature and was filtered to remove solid impurities. KPF_6 (.2333 g, 1.267 mmol) was added to the red-orange filtrate and the solution was reduced in volume to ~15 mL on a rotary evaporator. The desired complex was precipitated by addition of diethyl ether dropwise into the solution. The dark-red solid was collected on fine glass frit, washed with 30 mL of diethyl ether, and dried in vacuo.

The compound was purified by column chromatography. The crude compound (.400 g) was redissolved in a minimum quantity of CH_3CN and chromatographed on an alumina column (4 inches x 2.7 cm) previously developed with CH_3CN. The sample was loaded on the column with CH_3CN followed by 20 mL of reagent acetone. At this point, pink and green impurity bands were observed. The main product was eluted (as an orange band) with a 1:3 CH_2Cl_2 / CH_3CN solution. Three distinct impurity bands remained on the column after elution. A band stuck to the top of the column and changed from dark brown to purple when the solvent was switched from CH_3CN to acetone. A dark orange band was noticed trailing the main cut. The eluent was reduced to 10 mL and diethyl ether was added dropwise to precipitate the compound. The compound was isolated by use of a fine glass frit, washed with 30 mL of diethyl ether, and dried in vacuo. Yield : 0.218 g, 43% based on $Ru^{II}(bpy)_2Cl_2 \cdot 2H_2O$.

$[Ru^{II}(bpyrm)_2(bpy)](PF_6)_2$ - The procedure developed by Rillema[6] and coworkers was followed with some modifications. In a typical preparation $Ru(bpy)Cl_4$ (.399 g, 1 mmol) and bpyrm (.949 g, 6 mmol) were suspended in 20 mL of ethylene glycol. Upon heating and stirring at reflux for 30 minutes, the

blue-green solution turned to a red-orange color. The solution was cooled to room temperature. About 3 mL of an aqueous, saturated KPF_6 solution was then added to precipitate the orange complex as the hexafluorophosphate salt. After 20 mL of water was added, the precipitate was collected on a fine glass frit, redissolved in a minimum of CH_3CN, and then precipitated by addition of diethyl ether dropwise to the solution. The crude compound was dried in vacuo.

The compound was redissolved in a minimum quantity of CH_3CN and chromatographed on an alumina column (4 inches x 4.5 cm) previously developed with CH_3CN. The main product (an orange band) was separated with a very slow drop rate from a brown band at the top of the column. The eluent was then rotary evaporated to ~7 mL and was precipitated by addition of diethyl ether dropwise into the solution. The orange solid was collected on a fine glass frit, washed with 30 mL of diethyl ether, and dried in vacuo.
Yield : 0.440g, 51%.

[cis-$Ru^{III}(NH_3)_4Cl_2$]Cl - The procedure of Clarke[7] and coworkers was followed with slight modification. In a typical preparation $[Ru^{III}(NH_3)_5Cl]Cl_2$ (1.90 g, 6.49 mmol) (purchased or prepared from $[Ru^{II}(NH_3)_6]Cl_2$ following the procedure of Vogt[7] and coworkers) was added to 19 mL of water. The solution was heated to 55 °C with a water bath and 2,3-dihydroxynaphthalene (H_2dhn) (2.07 g, 12.9 mmol) which had been dissolved in 17 mL of 1:1 water-ethanol at 55 °C, was added with constant stirring. The reaction mixture was adjusted to pH 9.5 with fresh 3 M NaOH. The solution turned a deep blue and was heated for an additional 40 minutes. The reaction mixture was filtered on #1 filter paper and evaporated to dryness on a rotary evaporator in a 400 mL round bottom flask (care must be taken to avoid foaming of solution). The blue residue was scraped out of the flask and the solid remaining in the flask was removed by

dissolution in a minimum quantity of water. All of the solid product was combined and dissolved in a minimum quantity of water. Concentrated HCl (15 mL) was added and the mixture was stirred and heated to 50 °C for 15 minutes. The red-violet solution was allowed to cool to room temperature and a white solid impurity (H_2dhn) was filtered out. The solution was then extracted three times with 15 mL portions of CH_3Cl in a separatory funnel. The aqueous (violet) layer was transferred to a beaker and an equal volume of absolute ethanol was added (~30 mL). The solution was refrigerated (~5 °C) for two hours, and the product precipitated out as a flocculent dull yellow solid. The product was collected on a fine glass frit, washed with CH_3Cl, ethanol, and diethyl ether, and then dried in vacuo. Yield of crude product : 0.748 g, 42%.

The compound was purified by dissolving the crude product in a minimum amount of concentrated HCl (care must be taken to avoid using an excess amount of HCl) followed by addition of three volumes of absolute ethanol and then cooling the solution in a freezer at -2°C to facilitate the precipitation of a fine yellow solid. Overall yield : 0.524 g, 29%.

$[Ru^{II}(bpy)_2(bpyrm)Ru^{II}(NH_3)_4](PF_6)_4$ - In a typical preparation $[Ru^{II}(bpy)_2(bpyrm)](PF_6)_2 \cdot H_2O$ (.100 g, .114 mmol) and $[Ru^{III}(NH_3)_4Cl_2]Cl$ (.095 g, .345 mmol) were added to two separate 3-necked flasks containing 40 mL of reagent acetone and 20 mL of water respectively. Both flasks (and solvents) had previously been deaerated for 30 minutes with argon. The two flasks were connected via a stainless steel cannula while an inert atmosphere was maintained. The argon gas was passed through a solution of reagent acetone via a bubble frit prior to reaching the reaction vessels. See Figure 2-1.

After the reactants were added to their respective flasks they were allowed to stir under argon for 20 minutes. The red-orange $[Ru^{II}(bpy)_2(bpyrm)](PF_6)_2$

Figure 2-1 : Experimental set-up for synthesis of $[Ru^{II}(bpy)_2(bpyrm)Ru^{II}(NH_3)_4](PF_6)_4$ and $[Ru^{II}(bpy)\{(bpyrm)Ru^{II}(NH_3)_4\}_2](PF_6)_6$.

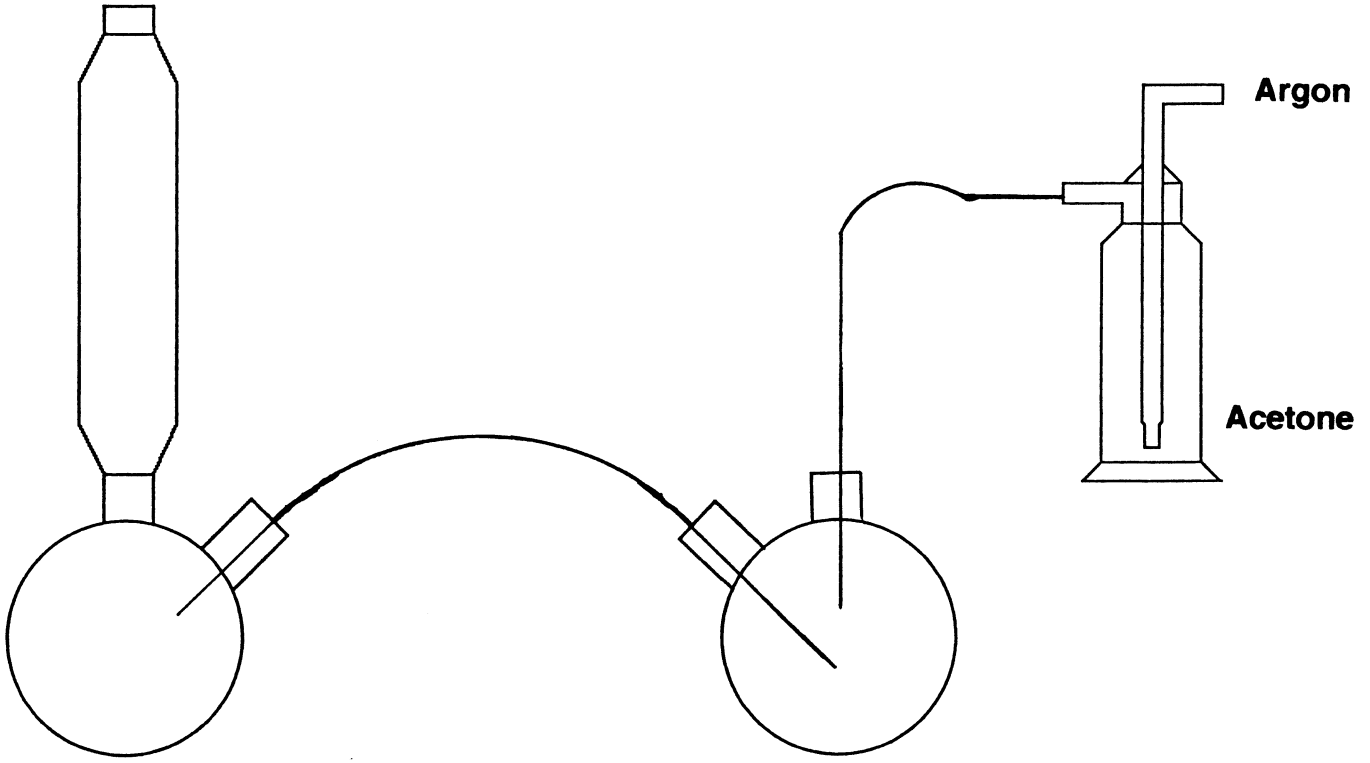

- acetone solution was heated to 40°C, while Zn/Hg amalgam[8] was added to the solution containing $[Ru^{III}(NH_3)_4Cl_2]^+$ monomer and allowed to react for 30 minutes. As the $[Ru^{III}(NH_3)_4Cl_2]^+$ species was reduced to $[Ru^{II}(NH_3)_4(H_2O)_2]^{2+}$ the color changed from a pale creme to a characteristic golden yellow. The $[Ru^{II}(NH_3)_4(H_2O)_2]^{2+}$ was transferred via cannula under argon to the solution containing $Ru^{II}(bpy)_2(bpyrm)$ upon which the resulting mixture immediately changed to a very dark green-blue color. The mixture was stirred under argon at 40°C for 2 hours.* The solution was then rotary evaporated to ~10 mL and the crude product was precipitated by the dropwise addition of a saturated solution of NH_4PF_6 while cooling in an ice bath. The green solid was collected on a fine glass frit, washed with a few drops of cold water and dried in vacuo.
Yield : 168 mg.

The crude sample was then dissolved with stirring in 20 mL of reagent acetone, and then filtered through a fine glass frit to remove a small amount of insoluble solid. A 70/30 methanol/acetone saturated solution of TEAC was added dropwise to the solution to precipitate the dimer as the chloride salt (it is important not to add too much TEAC). The green precipitate was collected on a fine glass frit and washed with cold acetone until the filtrate no longer showed signs of the unreacted $[Ru^{II}(bpyrm)(bpy)_2]^{2+}$ which has a characteristic yellow-orange color. The solid was then dried in vacuo. Yield : 131 mg.

The chloride salt of the dimer was then redissolved in 5 mL of water and filtered through a 2 mL fine glass frit to remove insoluble impurities. The dimer was then reprecipitated as the PF_6^- salt by the dropwise addition of a saturated solution of NH_4PF_6 while cooling in an ice bath. The dimer was then collected on a fine glass frit, washed with a few drops of cold water, diethyl ether, and finally dried in vacuo.

* Appendix I details numerous attempts to optimize the synthetic procedure.

The process of "salt-switching" was then repeated twice more in order to remove the majority of unreacted monomers and reaction side products. Yield : 119 mg. Overall Yield : 54%. Calculated. for $[Ru^{II}(bpy)_2(bpyrm)Ru^{II}(NH_3)_4](PF_4)_4$:

Calc'd : C, 25.46; H, 2.59; N, 12.73.

Found : C, 21.38; H, 2.97; N, 13.96. .

$[Ru^{II}(bpy)\{(bpyrm)Ru^{II}(NH_3)_4\}_2](PF_6)_6$ - The trimer was prepared in a similar manner as the dimer. In a typical preparation $[Ru^{II}(bpyrm)_2(bpy)](PF_6)_2$ (.100 g, .116 mmol) and $[Ru^{III}(NH_3)_4Cl_2]Cl$ (.191 g, .695 mmol) were added to two separate 3-necked flasks containing 50 mL of reagent acetone and 20 mL of water respectively. Both flasks and solvents had previously been deaerated for 30 minutes with argon. The two flasks were connected via a stainless steel cannula while an inert atmosphere was maintained. The argon gas was passed through a solution of reagent acetone via a bubble frit prior to reaching the reaction vessels. See Figure 2-1.

The reactants were allowed to stir under argon for 30 minutes. The red-orange $[Ru^{II}(bpyrm)_2(bpy)](PF_6)$/acetone solution was heated to 40°C, while Zn/Hg amalgam[8] was added to the solution containing $[Ru(NH_3)_4(Cl)_2]^+$ and allowed to react for 30 minutes. The $[Ru^{II}(NH_3)_4(H_2O)_2]^{2+}$ produced was transferred over via cannula under argon to the solution containing $[Ru^{II}(bpyrm)_2(bpy)]^{2+}$ upon which the resulting mixture immediately changed to a very dark green-blue color. The mixture was stirred under argon at 40°C for 2 hours.* The solution was then rotary evaporated to ~10 mL and the crude product was precipitated by the dropwise addition of a saturated solution of NH_4PF_6 while cooling in an ice bath. The green solid was collected on a fine

glass frit, washed with a few drops of cold water and dried in vacuo.
Yield : 354 mg.

The crude trimer was then dissolved with stirring in 20 mL of reagent acetone, and then filtered through a fine glass frit to remove a small amount of insoluble solid. A 70/30 methanol/acetone saturated solution of TEAC was added dropwise to the solution to precipitate the trimer as the chloride salt. The green precipitate was collected on a fine glass frit and washed with cold acetone until the filtrate no longer showed signs of the unreacted $[Ru^{II}(bpyrm)_2(bpy)]^{2+}$ which has a characteristic red-orange color. The solid was then dried in vaccuo.
Yield : 168 mg.

The chloride salt of the trimer was then redissolved in 5 mL of water and filtered through a 2 mL fine glass frit to remove insoluble impurities. The trimer was then reprecipitated as the PF_6^- salt by the dropwise addition of a saturated solution of NH_4PF_6 while cooling in an ice bath. The trimer was then collected on a fine glass frit, washed with a few drops of cold water, diethyl ether, and finally dried in vacuo.

The process of "salt-switching" was then repeated twice more in order to remove the majority of unreacted monomers and reaction side products.
Yield : 196 mg. Overall Yield : 76%.
Calculated. for $Ru^{II}(bpy)\{(bpyrm)Ru^{II}(NH_3)_4\}_2](PF_4)_6$:

Calc'd : C, 17.53; H, 2.59; N, 12.73.

Found : C, 13.54; H, 2.77; N, 13.16.

*Appendix II details numerous attempts to optimize the synthetic procedure.

References

(1) Krause, R. A. *Inorg. Chim. Acta.* **1977**, *22*, 209-213.

(2) Sullivan, B. P., The University of North Carolina at Chapel Hill, personal communication, 1990.

(3) Sullivan, B. P.; Salmon, D. J.; Meyer, T. J. *Inorg. Chem.* **1978**, *17*, 3334-3341.

(4) Sprintschnik, G.; Sprintschnik, H. W.; Kirsch, P. P.; Whitten, D. G. *J. Am. Chem. Soc.* **1977**, *99*, 4947-4954.

(5) Rillema, D. P.; Mack, K. B. *Inorg. Chem.* **1982**, *21*, 3849-3854.

(6) Rillema, D. P.; Allen, G.; Meyer, T. J.; Conrad, D. *Inorg. Chem.* **1983**, *22*, 1617-1622.

(7) Pell, S. D.; Sherban, M. M.; Tramontano, V.; Clarke, M. J. In *Inorg. Synth.* ; Kaesz, H. D. Ed.; John Wiley & Sons: New York, **1989**, *26*, 65-68.

(8) *Handbook of Preparative Inorganic Chemistry Vol. II* ; Brauer, G., Ed.; Academic: New York, **1965**, 1806-7.

Results and Discussion

Characterization of Starting Materials

cis-$Ru^{II}(bpy)_2Cl_2 \cdot 2H_2O$ - The UV-vis spectrum (Figure 3-1) was taken in CH_3CN and the following absorption maxima were observed : 551.0 nm and 377.0 nm ($d\pi[Ru^{II}] \rightarrow \pi^*[bpy]$ MLCT) and 241.0 nm and 297.0 nm (both bpy $\pi \rightarrow \pi^*$). The $d\pi[Ru^{II}] \rightarrow \pi^*[bpy]$ transitions are formally called metal-to-ligand charge transfer (MLCT) bands. The transitions are assigned from the work of Crutchley and Lever[1a] (and references therein).

Table 3-1 compares the observed absorbance maxima (and absorption coefficients, ϵ) with those found by Crutchley and Lever[1a]. The ϵ values for this work were determined using only a single concentration. The two waters of hydration are included on the basis of previous literature results[1b] and the similarity of the observed ϵ values with those from ref. 1a.

A cyclic voltammogram (Figure 3-2) in 0.1M TBAH/CH_3CN showed a reversible Ru(III)/Ru(II) couple at $E_{1/2}$ = 0.326 V vs. SSCE. The literature value[1], 0.31 V, was taken in 0.1M TEAP/CH_3CN vs. SSCE (Table 3-2).

[$Ru^{II}(bpy)_2(bpyrm)$]$(PF_6)_2 \cdot H_2O$ - The UV-vis spectrum (Figure 3-3) was taken in CH_3CN, and the following absorptions were observed (transitions assigned according to the work of Rillema[2] and Meyer[3] - see Table 3-1) : 423.0 nm ($d\pi[Ru^{II}] \rightarrow \pi^*[bpyrm]$ MLCT), 361.0 nm ($d\pi[Ru^{II}] \rightarrow \pi^*[bpy]$ MLCT), 288.0 nm (ligand $\pi \rightarrow \pi^*$) and 239.0 nm (ligand $\pi \rightarrow \pi^*$). The low energy shoulder at 472.0 nm is most likely due to a MLCT transition to the more easily reduced bipyrimidine ligand.

The ϵ values (determined from a single concentration), compare quite well with the literature values. Therefore, the complex is written with one water of hydration, as in ref. 2 .

A cyclic voltammogram (Figure 3-4) in 0.1M TEAP/CH_3CN displayed a reversible Ru(III)/Ru(II) couple at $E_{1/2}$ = 1.372 V vs. SSCE. This compares to 1.40 V reported by Rillema[2] in the same medium[4] (Table 3-2).

$[Ru^{II}(bpyrm)_2(bpy)](PF_6)_2$ - The UV-vis spectrum (Figure 3-5) was taken in CH_3CN and the following absorptions were observed (transitions assigned according to the work of Meyer and Rillema[3] - see Table 3-1) : 458.0 nm (sh), 420.0 nm, 369.0 nm and 330.0 nm (overlapping ($d\pi[Ru^{II}]$ --> π^*[bpy/bpyrm]) MLCT bands); 283.5 nm and 258.0 nm (both ligand π --> π^*).

Although the absorption maxima from this work and ref. 3 show fair agreement, the ϵ values reported for this work appear to be consistently low. This could be due (in part) to waters of hydration present in this preparation. Another possible explanation might be contamination by an "inert" material such as excess salt (NH_4PF_6) which would lower the calculated ϵ values.

The cyclic voltammogram (Figure 3-6) in 0.1M TEAP/CH_3CN displayed a reversible, one electron Ru(III)/Ru(II) couple at $E_{1/2}$ = 1.501 V vs. SSCE. This compares to 1.55 V reported by Meyer and Rillema[3] in the same medium[4] (Table 3-2).

$[Ru^{III}(NH_3)_4Cl_2]Cl$ - The UV-vis spectrum (Figure 3-7) was taken in water and the following absorptions were observed (transitions assigned according to the work of Clarke[5a] and Ford[5b] - see Table 3-1) : 342.5.0 nm and 301.0 nm (both ligand-to-metal-charge-transfer bands, LMCT); 251.0 nm (ligand π --> π^*).

As can be observed from Table 3-1, there is a consistent 7 - 9 nm difference between the absorption maxima reported here and those in ref. 5 (due to inaccurate instrument calibration). However, ϵ values for the maxima agree quite well with those in the literature.

A cyclic voltammogram (Figure 3-8), recorded in 0.1M KCl/H_2O vs. SSCE, showed irreversible behavior with peak separations of 263 mV between the cathodic and anodic waves - see Table 3-2. Ford[5c,d] has shown that when $[Ru^{III}(NH_3)_4Cl_2]^+$ is reduced to $Ru^{II}(NH_3)_4Cl_2$ in aqueous solution, a very rapid aquation reaction takes place. Therefore, unless the scan rate is extremely rapid, reoxidation (during the reverse sweep) of $[Ru^{II}(NH_3)_4(H_2O)_2]^{2+}$ takes place, and <u>not</u> reoxidation of $[Ru^{II}(NH_3)_4Cl_2]$. In fact, it was only at scan rates of 2.5 V/s that Ford[5c,d] was able to show reversible behavior for the $[Ru^{III}(NH_3)_4Cl_2]^+/[Ru^{II}(NH_3)_4Cl_2]^0$ couple. At lower scan rates, (~500 mV/s) irreversible behavior was observed (ie $[Ru^{III}(NH_3)_4Cl_2]^+/[Ru^{II}(NH_3)_4(H_2O)_2]^{2+}$).

In this work, the cyclic voltammogram of $[Ru^{III}(NH_3)_4Cl_2]^+$ was recorded at a scan rate of 100 mV/s, far slower than even the "slow" rate used by Ford[5c,d]. Therefore, it is expected that this work would show irreversible behavior for the complex, with a reduction peak (for $[Ru^{III}(NH_3)_4Cl_2]^+$) close to that reported by Ford[5c,d] and a reoxidation wave close to that reported for $[Ru^{II}(NH_3)_4(H_2O)_2]^{2+}$. The observed reduction peak (-0.369 V vs SSCE) compares well with that reported by Ford[5c,d] for $[Ru^{III}(NH_3)_4Cl_2]^+$ (-0.388 V vs SSCE) and the reoxidation wave (-0.106 V vs SSCE) agrees well with that reported for $[Ru^{II}(NH_3)_4(H_2O)_2]^{2+}$ (-0.118 V vs SSCE)[5c].

The overall reaction can thus be written as :

$$[Ru^{III}(NH_3)_4Cl_2]^+ (aq) + 1\ e \text{ -----> } [Ru^{II}(NH_3)_4Cl_2]^0$$

$$[Ru^{II}(NH_3)_4Cl_2]^0 \xrightarrow[-2\ Cl^-\ \ +2\ H_2O]{\text{rapid}} [Ru^{II}(NH_3)_4(H_2O)_2]^{2+}$$

$$[Ru^{II}(NH_3)_4(H_2O)_2]^{2+} \text{ -------> } [Ru^{III}(NH_3)_4(H_2O)_2]^{3+} + 1e$$

Characterization of bimetallic and trimetallic complexes

$[Ru^{II}(bpy)_2(bpyrm)Ru^{II}(NH_3)_4](PF_6)_4$ - [2,2] form : The UV-vis spectrum (Figure 3-9) was taken in CH_3CN, and the absorption bands that were observed are listed in Table 3-3 along with transition assignments. The MLCT bands and other transitions were assigned on the basis of the intensities and energies of previously reported[6,7] Ru(II)-ammine and Ru(II)-bipyridine(bpy) complexes.

As seen in Table 3-3, the transition observed at 687.0 nm is assigned as a low energy MLCT band, which arises from a transition (intramolecular ET) from the easily oxidized Ru(II)-ammine to the easily reduced bpyrm bridging ligand. This compares well with the low energy $d\pi[Ru^{II}\text{-ammine}] \rightarrow \pi^*[bpyrm]$ MLCT (697.0 nm) reported by Ruminski et al.[6] (in H_2O) for the bimetallic species $[Ru^{II}(NH_3)_4(bpyrm)Ru^{II}(NH_3)_4]^{4+}$. The absorption shoulder at 498.0 nm is assigned as a $d\pi[Ru^{II}\text{-bpy}] \rightarrow \pi^*[bpyrm]$ MLCT. This is red shifted compared to the equivalent transition (472.0 nm) assigned to $Ru^{II}(bpy)_2(bpyrm)^{2+}$ (Table 3-1). The red shift is probably due to coordination of the $-Ru^{II}(NH_3)_4^{2+}$ fragment to the bpyrm and subsequent lowering of the π^* energy level of the bpyrm ligand.

The absorption envelope centered at 423.0 nm in the bimetallic $[Ru^{II}(bpy)_2(bpyrm)Ru^{II}(NH_3)_4]^{4+}$ is assigned as arising from a summation of $d\pi[Ru^{II}\text{-bpy}] \rightarrow \pi^*[bpy]$ MLCT's, and a <u>second</u>, $d\pi[Ru^{II}\text{-ammine}] \rightarrow \pi^*[bpyrm]$ MLCT band. (Ruminski et al[6] reports both low and high energy MLCT bands for the bimetallic complex $[(NH_3)_4Ru^{II}(bpyrm)Ru^{II}(NH_3)_4]^{4+}$.)

The ultraviolet region of the spectrum of $[Ru^{II}(bpy)_2(bpyrm)Ru^{II}(NH_3)_4]^{4+}$ is characterized by intense absorption bands at 282.0 nm and 245.0 nm. These bands are characteristic of $\pi \rightarrow \pi^*$ transitions of the bpy and bpyrm ligands.[8]

Redox properties were determined by cyclic voltammetry, and the cyclic voltammogram (Figure 3-10 - three consecutive scans on the same sample) was taken in a CH_3CN solution containing 0.1 M TEAP as the supporting electrolyte. The $E_{1/2}$ values are listed in Table 3-5. A scan out to +1.550 V showed a fairly reversible wave (ΔE_p = 70 mV) centered at $E_{1/2}$ = +0.899 V. This wave is assigned as a one-electron (metal-centered) oxidation of the $(bpyrm)Ru^{II}(NH_3)_4^{2+}$ portion of the dimer. This compares with an $E_{1/2}$ = +0.66 V (ΔE_p = 58 mV) for $[(bpyrm)Ru^{II}(NH_3)_4](PF_6)_2$ in the same solvent (Table 3-5).[9] The +0.239 V shift in $E_{1/2}$ for $[Ru^{II}(bpy)_2(bpyrm)Ru^{II}(NH_3)_4]^{4+}$ is thus due to the effect of coordination of a second Ru^{II} center on the bridging bpyrm ligand.

A scan out to +1.900 V produced a second oxidation that was centered at $E_{1/2}$ = +1.626 V (ΔE_p = 128 mV). This is assigned as a one-electron (metal-centered) oxidation of the $(bpy)_2Ru^{II}(bpyrm)^{2+}$ portion of $[Ru^{II}(bpy)_2(bpyrm)Ru^{II}(NH_3)_4]^{4+}$.[9] This second oxidation wave was shifted anodically (harder to oxidize) from that measured for the monometallic complex $[Ru^{II}(bpy)_2(bpyrm)]^{2+}$ (Table 3-2) in the same solvent.[2,3] This anodic shift in $E_{1/2}$ is not surprising since the Ru^{II} center being oxidized at +1.6 V in the bimetallic complex would be attached to an electron deficient $-Ru^{III}(NH_3)_4^{3+}$ fragment.

Figure 3-10 also shows that the Ru^{III}/Ru^{III} species generated (at E > 1.6 v) was unstable, as a decomposition peak was observed in the reverse scan at +1.270 V. As shown in Figure 3-10, this decomposition wave was only observed if the complex was allowed to undergo a <u>second</u> oxidation to the Ru^{III}/Ru^{III} (or [3,3]) species. Ruminski et al[6] have reported that $[Ru^{II}(NH_3)_4(bpyrm)Ru^{II}(NH_3)_4]^{4+}$ also shows decomposition after a second oxidation to the [3,3] form. For $[Ru^{II}(bpy)_2(bpyrm)Ru^{II}(NH_3)_4]^{4+}$, the

decomposition peak is very close to the reduction potential reported for $[Ru^{III}(bpy)_2(bpyrm)]^{3+}$ in Table 3-2. Therefore, decomposition can be attributed to the cleavage of the dimer into two monomeric species:

$$[(bpy)_2Ru^{III}(bpyrm)Ru^{III}(NH_3)_4]^{6+} \rightarrow [(bpy)_2Ru^{III}(bpyrm)]^{3+} + [Ru^{III}(NH_3)_4(CH_3CN)_2]^{3+}$$

(caused by bridge rupture to yield monometallic species)

and/or

$$[(bpy)_2Ru^{III}(bpyrm)Ru^{III}(NH_3)_4]^{6+} \rightarrow [(bpy)_2Ru^{III}(CH_3CN)_2]^{3+} + [(bpyrm)Ru^{III}(NH_3)_4]^{3+}$$

Both $[(bpy)_2Ru^{III}(bpyrm)]^{3+}$ and $[(bpy)_2Ru^{III}(CH_3CN)_2]^{3+}$ would give reduction peaks in the +1.2 to +1.3 V range (vs SSCE).

Figure 3-10 also reveals two additional (and quite small) waves at ~0.7 V (on the anodic sweep) and ~0.6 V (on the reverse cathodic sweep). These peaks have been assigned as the oxidation and re-reduction of a small amount of impurity present. One possible source of this impurity could have been simply unreacted $[(NH_3)_4Ru^{II}(H_2O)_2]^{2+}$ which would probably take the form $[(NH_3)_4Ru^{II}(CH_3CN)_2]^{2+}$ in CH_3CN. Moreover, the cathodic wave at ~+0.6 V does appear to be slightly enhanced, and this could have been due to small amounts of $[(bpyrm)Ru^{II}(NH_3)_4]^{3+}$ present after bridge rupture of the bimetallic species at E > +1.6 V (the $E_{1/2}$ of $[(bpyrm)Ru^{II}(NH_3)_4]^{2+}$ in CH_3CN was previously measured to be +0.66 V vs SSCE).

Other evidence, however, suggests that the origin of the impurity is more complicated than simply the presence of either unreacted starting material or decomposition products from bridge rupture. First, repeated attempts to separate the impurity from the bimetallic species by both ion-exchange and

size exclusion chromatography failed. This implies that the problem species is of similiar size and charge to that of the bimetallic complex. Secondly, when a control experiment was performed where the preparation of the bimetallic complex was carried out without addition of $[Ru^{II}(bpy)_2(bpyrm)](PF_6)_2$, the $[Ru^{II}(NH_3)_4(H_2O)_2]^{2+}$ species generated was observed to undergo several color changes even in the absence of O_2 . In fact, $[Ru^{II}(NH_3)_4(H_2O)_2]^{2+}$, generated in the absence of O_2 by reduction over Zn-amalgam, is known to be unstable.[5e] Third, elemental analysis of $[Ru^{II}(bpy)_2(bpyrm)Ru^{II}(NH_3)_4](PF_4)_4$ consistently showed low carbon.

Calc'd : C, 25.46; H, 2.59; N, 12.73.

Found : C, 21.38; H, 2.97; N, 13.96.

The above information seems to imply that the impurity could have been some sort of bimetallic Ru-ammine species (lacking any polypyridyl ligands) formed from a competing side-reaction (decomposition) of the $[(NH_3)_4Ru^{II}(H_2O)_2]^{2+}$ species generated during the preparation. This same impurity seems to appear in the preparation of the trimetallic species (vide infra) which was prepared by a very similiar procedure.

$[Ru^{II}(bpy)\{(bpyrm)Ru^{II}(NH_3)_4\}_2](PF_6)_6$ - [2,2,2] form : The UV-vis spectrum (Figure 3-11) was taken in CH_3CN, and the absorption bands that were observed are listed in Table 3-4 along with transition assignments. The assignments have been made based on comparisions with the bimetallic species $[Ru^{II}(bpy)_2(bpyrm)Ru^{II}(NH_3)_4]^{4+}$, and with the spectral assignments of previously reported analogous compounds.[6,7]

The transition observed at 694.0 nm can be assigned as a $d\pi$ [Ru^{II}-ammine] --> π^*[bpyrm] MLCT band. This represents a slight red-shift from the equivalent absorption in the bimetallic species. It could be argued that this small shift is due to each bpyrm feeling the effects of two Ru^{II} centers

(one adjacent and one remote), thus lowering the π^* LUMO energy slightly. This point can not be pressed, however, since the broad low absorption represented here may cause some uncertainty in exact peak maximum. What is significant about the maximum at 694 nm for the trimetallic species is that its absorptivity value is approximately double that of the bimetallic species (Table 3-3). This is exactly what would be expected (ie. two $d\pi$ [Ru^{II}-ammine] --> π^*[bpyrm] transitions per molecule).

The absorption envelope centered at 435.0 nm most likely arises from overlapping transitions assigned as $d\pi$[Ru^{II}-bpy] --> π^*[bpy] MLCT , $d\pi$[Ru^{II}-bpy] --> π^*[bpyrm] MLCT ,and $d\pi$ [Ru^{II}-ammine] --> π^*[bpyrm] "high-energy" MLCT bands. The shift of the maximum of this absorption envelope to lower energy is consistent with a lowering of energy of the π^* LUMO's of bpyrm in the trimetallic species (as compared to the bimetallic complex). This is the same conclusion that was hinted at from the shift (687 --> 694 nm) mentioned previously.

As in the bimetallic complex, the trimetallic species also exhibits intense ultraviolet absorption bands (272.0 nm and 246.0 nm). These bands are characteristic of π --> π^* transitions of the bpy and bpyrm ligands.[8]

Redox properties were determined by cyclic voltammetry, and the cyclic voltammogram (Figure 3-12) was taken in a CH_3CN solution containing 0.10 M TEAP as the supporting electrolyte. The results are listed in Table 3-5. A scan out to +1.300 V showed a wave (ΔE_p = 100 mV) centered at $E_{1/2}$ = +0.917 V. This wave is assigned as a one-electron (metal-centered) oxidation of each of the (bpyrm)$Ru^{II}(NH_3)_4^{2+}$ portions of the complex (net two-electron process). The measured peak separation (ΔE_p = 100 mV) is much larger than expected for a reversible, two-electron process (30 mV). Therefore, it seems likely that this oxidation wave is actually formed as a result of two very closely spaced,

sequential one-electron oxidations of each end of the trimetallic complex. Scans out to +1.900 V revealed no new oxidation waves. Apparently, the central -[(bpyrm)Ru^{II}(bpy)(bpyrm)]- "bridging" complex is much more difficult to oxidize than the monometallic $Ru^{II}(bpyrm)_2(bpy)^{2+}$ ($E_{1/2}$ = +1.50 V) due to the fact that the bridging complex is attached to two electron deficient -$Ru^{III}(NH_3)_4^{3+}$ fragments.

As in the bimetallic species, Figure 3-12 also shows that the $[Ru^{II}(bpy)\{(bpyrm)Ru^{II}(NH_3)_4\}_2]^{6+}$ solution was contaminated with an easily oxidized impurity. Since the methods of preparation for the bimetallic and trimetallic complexes were similiar, it is reasonable to assume that it is a similiar impurity (arising from side reactions of $Ru^{II}(NH_3)_4(H_2O)_2^{2+}$ and containing no bpyrm). The elemental analysis of $[Ru^{II}(bpy)\{(bpyrm)Ru^{II}(NH_3)_4\}_2](PF_4)_6$, shown below, is consistent with this (low carbon). Once again, rigorous attempts at purification, documented in the experimental section and in the appendices, failed to yield a sample of analytical purity.

Calculated. for $Ru^{II}(bpy)\{(bpyrm)Ru^{II}(NH_3)_4\}_2](PF_4)_6$:

Calc'd : C, 17.53; H, 2.59; N, 12.73.

Found : C, 13.54; H, 2.77; N, 13.16.

Generation and Characterization of Mixed-Valence Complexes

$[Ru^{II}(bpy)_2(bpyrm)Ru^{III}(NH_3)_4]^{5+}$ - [2,3] form :

$[Ru^{II}(bpy)_2(bpyrm)Ru^{III}(NH_3)_4]^{5+}$, referred to as [2,3], was produced by exhaustive oxidation of $[Ru^{II}(bpy)_2(bpyrm)Ru^{II}(NH_3)_4]^{4+}$ in 0.1M TBAH/CH_3CN at a Pt mesh electrode (+1.200 V vs SSCE) using a quartz cell fused to a three compartment electrochemical cell (University of North Carolina at Chapel Hill - Chemistry Department Glass Shop). All of the data collected for the [2,2] and

[2,3] ions were from freshly prepared solutions and were taken over relatively short time periods (30 - 60 minutes). Re-reduction of the [2,3] ion back to [2,2] (0.0 V vs SSCE) resulted in ≥ 75% recovery of $[Ru^{II}(bpy)_2(bpyrm)Ru^{II}(NH_3)_4]^{4+}$, based on absorption measurements.

The UV-vis spectrum of the mixed-valence complex [2,3] (Figure 3-13) was characterized by the loss of the low energy MLCT band ($d\pi[Ru^{II}$-ammine] --> π^*[bpyrm]) found at 697.0 nm in the [2,2] complex. This was an expected result based on the fact that at +1.2 V the Ru^{II}-ammine portion of the complex has been oxidized to Ru^{III}-ammine (Figure 3-10). The $d\pi[Ru^{II}$-bpy] --> π^*[bpyrm] MLCT band at 498.0 nm in the [2,2] form was red shifted to 581.0 nm in the [2,3] complex. This shift was due to the lowering of the energy of the π^* orbital on bpyrm due to its attachment to Ru^{III} (Table 3-6). In addition, the absorption envelope centered at 423.0 nm in the [2,2] ion showed a loss of intensity (and an apparent blue-shift to 411.0 nm) due to loss of the second $d\pi[Ru^{II}$-ammine] --> π^*[bpyrm] MLCT band.[9]

An intervalence charge-transfer (IVCT) transition would be possible for $[Ru^{II}(bpy)_2(bpyrm)Ru^{III}(NH_3)_4]^{5+}$. Using data for the asymmetric mixed-valence species $[Ru^{II}(bpy)_2Cl$-pyrazine-$Ru^{III}(NH_3)_5]^{5+}$ reported by Meyer et al.[10], we can estimate where the IVCT band for the [2,3] dimer should be observed.

The energy of the IVCT band (E_{op}) for an asymmetric mixed-valence species can be estimated[9] as :

$$E_{op} = \Delta E_o + E_{FC} \qquad (1)$$

where ΔE_o is the difference in internal energy between the thermally equilibrated ion $[Ru^{II}(bpy)_2(bpyrm)Ru^{III}(NH_3)_4]^{5+}$ and its oxidation state isomer

$[Ru^{III}(bpy)_2(bpyrm)Ru^{II}(NH_3)_4]^{5+}$, and E_{FC} is the Franck-Condon energy (E_{FC} = $E_r = E_{in} + E_{out}$ = total reorganization energy).[10] ΔE_o can now be written as:

$$\Delta E_o = E_{1/2}\{[Ru^{III}(bpy)_2(bpyrm)Ru^{II}(NH_3)_4]^{5+} \text{ --> } [Ru^{II}(bpy)_2(bpyrm)Ru^{II}(NH_3)_4]^{4+}\} -$$
$$E_{1/2}\{[Ru^{II}(bpy)_2(bpyrm)Ru^{III}(NH_3)_4]^{5+} \text{ --> } [Ru^{II}(bpy)_2(bpyrm)Ru^{II}(NH_3)_4]^{4+}\} \quad (2)$$

or as : $$\Delta E_o = E_1 - E_2 . \quad (3)$$

E_2 has been measured to be +0.899 V vs SSCE (Table 3-5), and E_1 can be estimated from the $E_{1/2}$ value of the symmetrical dimer $[Ru^{II}(bpy)_2(bpyrm)Ru^{II}(bpy)_2]^{4+}$; E_1 = +1.49 V vs SSCE (the average of values reported in refs 7 and 11). Therefore, $\Delta E_o = E_1 - E_2$ = +0.591 V. E_{FC} can be estimated from the observed IVCT band (in CH_3CN) reported by Meyer et al.[10] for $[Ru^{II}(bpy)_2Cl\text{-pyrazine-}Ru^{III}(NH_3)_5]^{5+}$ where E_{FC} = 8000 cm^{-1}. From this data E_{op} for $[Ru^{II}(bpy)_2(bpyrm)Ru^{II}(NH_3)_4](PF_6)_4$ can be estimated as 1.28 x 10^4 cm^{-1} or 780 nm. An extremely low intensity IVCT band could be hidden (in the 600-800 nm range) by the long-wavelength tail of the 581.0 nm band in Figure 3-13 or could be indistinguishable from residual absorption of unoxidized $[Ru^{II}(bpy)_2(bpyrm)Ru^{II}(NH_3)_4]^{4+}$ around 700 nm. However, scans out to ~1600 nm revealed no evidence for an IVCT transition.

$[Ru^{II}(bpy)\{(bpyrm)Ru^{III}(NH_3)_4\}_2]^{8+}$ - [3,2,3] form :

$[Ru^{II}(bpy)\{(bpyrm)Ru^{III}(NH_3)_4\}_2]^{8+}$, referred to as [3,2,3], was produced by exhaustive oxidation of $[Ru^{II}(bpy)\{(bpyrm)Ru^{II}(NH_3)_4\}_2]^{6+}$ in 0.1M TEAP/CH_3CN at a Pt mesh electrode (+1.150 V vs SSCE). Re-reduction of the [3,2,3] ion back to [2,2,2] at 0.0 V vs SSCE resulted in ≥ 95% recovery of $[Ru^{II}(bpy)\{(bpyrm)Ru^{II}(NH_3)_4\}_2]^{6+}$ based on absorption measurements.

The UV-vis spectrum of the mixed-valence complex [3,2,3] (Figure 3-14) was characterized by the loss of the low energy MLCT band ($d\pi[Ru^{II}$-ammine] --> π^*[bpyrm]) found at 694.0 nm in the [2,2,2]. Also, there was a red-shifting of the $d\pi[Ru^{II}$-bpy] --> π^*[bpyrm] MLCT band from ~490.0 nm (in the [2,2,2] complex) to 533.0 nm (in the [3,2,3] complex); (Table 3-7). It should be noted that the absorption coefficient of this transition (6.4×10^{-3} M^{-1} cm^{-1}) was found to be approximately double that of the same transition in the [2,3] species (2.6×10^{-3} M^{-1} cm^{-1}). This further supports the assertion that the trimetallic species $[Ru^{II}(bpy)\{(bpyrm)Ru^{III}(NH_3)_4\}_2]^{8+}$ was actually synthesized since this structure would have two areas from which this transition could occur. The total absorption intensity in the 400 nm region of the [3,2,3] species was much less intense when compared to the [2,2,2] spectrum. This was due to the loss of the second (higher energy) $d\pi[Ru^{II}$-ammine] --> π^*[bpyrm] MLCT band which arises from both ends of the [2,2,2] species.

An IVCT transition for $[Ru^{II}(bpy)\{(bpyrm)Ru^{III}(NH_3)_4\}_2]^{8+}$ in CH_3CN is theoretically possible. The IVCT band in this [3,2,3] species would arise from the transition of an electron from the "center" ruthenium (Ru^{II}_c) to either one of the "terminal" ruthenium's (Ru^{III}_t) :

$$d\pi[\text{-}(bpyrm)Ru^{II}(bpy)(bpyrm)\text{-}] \text{ --> } d\pi[\text{-}Ru^{III}(NH_3)_4]$$

$$Ru_c \text{ --> } Ru_t \text{ IVCT} \quad .$$

It is possible to predict where this IVCT band might occur by viewing the symmetric trimetallic complex as an "asymmetric" bimetallic species :

$$[Ru^{III}(NH_3)_4(bpyrm)Ru^{II}(bpy)(bpyrm)] - [\text{-}Ru^{III}(NH_3)_4] \; .$$

From Eq. 1 : $E_{op} = \Delta E_o + E_{FC}$

$$\Delta E_o = E_{1/2}\{\,[3,3]\text{-}[2] \;\text{-->}\; [3,2]\text{-}[2]\,\} - E_{1/2}\{\,[3,2]\text{-}[3] \;\text{-->}\; [3,2]\text{-}[2]\,\} \qquad (4)$$

where :

$$[3,3]\text{-}[2] = [Ru^{III}(NH_3)_4(bpyrm)Ru^{III}(bpy)(bpyrm)] - [\text{-}Ru^{II}(NH_3)_4]$$

$$[3,2]\text{-}[3] = [Ru^{III}(NH_3)_4(bpyrm)Ru^{II}(bpy)(bpyrm)] - [\text{-}Ru^{III}(NH_3)_4]$$

$$[2,2]\text{-}[2] = [Ru^{II}(NH_3)_4(bpyrm)Ru^{II}(bpy)(bpyrm)] - [\text{-}Ru^{II}(NH_3)_4]\,,$$

or simply : $$\Delta E_o = E_1 - E_2\,. \qquad (5)$$

E_2 has been measured to be +0.917 V vs SSCE (Table 3-5). E_1 is estimated to be ~+1.95 V vs SSCE, which is the solvent limit in the cyclic voltammogram of the trimetallic species in Figure 3-12. Therefore, $\Delta E_o = E_1 - E_2 \approx +1.03$ V, and for $[Ru^{II}(bpy)\{(bpyrm)Ru^{III}(NH_3)_4\}_2]^{8+}$:

$$E_{op} \approx 1.03\ V + E_{FC} \qquad (6)$$

E_{FC} can be estimated from the observed IVCT bands (in CH_3CN) reported by Scandola et al.[12] for :

$$[\text{pyridine}(NH_3)_4Ru^{III}\text{-NC-}Ru^{II}(bpy)_2\text{-CN-}Ru^{III}(NH_3)_4\text{pyridine}]^{6+}$$

for this complex : $$E_{op} = \Delta E_o + E_{FC} = 13{,}600\ cm^{-1} \qquad (7)$$

$$\Delta E_o = E_{1/2}\{[3,3,2] \;\text{-->}\; [3,2,2]\} - E_{1/2}\{[3,2,3] \;\text{-->}\; [3,2,2]\} \qquad (8)$$

<u>or</u>

$$\Delta E_o = E_1 - E_2$$

[3,3,2] = [pyridine$(NH_3)_4Ru^{III}$-NC-$Ru^{III}(bpy)_2$-CN-$Ru^{II}(NH_3)_4$pyridine]$^{6+}$

[3,2,3] = [pyridine$(NH_3)_4Ru^{III}$-NC-$Ru^{II}(bpy)_2$-CN-$Ru^{III}(NH_3)_4$pyridine]$^{6+}$

[3,2,2] = [pyridine$(NH_3)_4Ru^{III}$-NC-$Ru^{II}(bpy)_2$-CN-$Ru^{II}(NH_3)_4$pyridine]$^{5+}$.

From data reported by Scandola et al.[12], $E_2 \approx +0.15$ V and an estimated upper limit for $E_1 \approx +1.35$ V.

$$\Delta E_o = E_1 - E_2 = +1.35 \text{ V} - 0.15 \text{ V} = +1.20 \text{ V} \quad . \tag{9}$$

In order to simplify units +1.20 V can be converted to 9671 cm^{-1} (1 V = 8065.48 cm^{-1}). From Eq. 7 :

$$E_{op} = \Delta E_o + E_{FC} = 13{,}600 \text{ cm}^{-1}$$

$$= 9671 \text{ cm}^{-1} + E_{FC} = 13{,}600 \text{ cm}^{-1}$$

$$E_{FC} = 3921 \text{ cm}^{-1} \quad . \tag{10}$$

The measured E_{FC} value for Scandola's trimetallic [3,2,3] complex can now be substituted into Eq. 6 :

$$E_{op} = 1.033 \text{ V} + E_{FC}$$

$$= 8332 \text{ cm}^{-1} + 3921 \text{ cm}^{-1}$$

$$= 1.23 \times 10^4 \text{ cm}^{-1}$$

$$= 816 \text{ nm} \quad .$$

Therefore, $\lambda_{IVCT} \approx 816$ nm for the Ru^{II}_c --> Ru^{III}_t IVCT band for the mixed-valence trimetallic complex $[Ru^{II}(bpy)\{(bpyrm)Ru^{III}(NH_3)_4\}]^{8+}$.

A definitive absorption ~800 nm was <u>not</u> observed for the [3,2,3] species. If the IVCT band did exist, it could remain undetected for reasons similiar to that given for the [2,3] bimetallic complex :

1) Extremely low absorption coefficient.

2) The band could be hidden under residual absorption around 700 nm from unoxidized [2,2,2] .

$[Ru^{II}(bpy)\{(bpyrm)Ru^{II/III}(NH_3)_4\}_2]^{8+}$ - [2,2,3] form :

Electrochemical and/or chemical oxidation of the [2,2,2] trimetallic complex to the one-electron oxidized [2,2,3] mixed-valence species was not attempted. Generation of and subsequent UV-Vis-NIR measurements on this species would obviously be necessary to test for "end-to-end" IVCT. However, generation of such a species requires precise knowledge of the concentration of the original [2,2,2] form in solution. Since the [2,2,2] form was never obtained in an analytically pure form, the partial oxidation was not carried out. An exact knowledge of concentration was not as necessary for generation of the [3,2,3] species, described in earlier sections.

Future Directions

Obviously the first order of business would be to find a purification method that would yield analytically pure samples of the bimetallic and trimetallic complexes. An analytically pure sample of the bimetallic species has recently been obtained[9] by restructuring the synthetic scheme. With this new method, $[Ru^{III}(NH_3)_4Cl_2]Cl$ was replaced with $[Ru^{II}(NH_3)_4(bpyrm)](PF_6)_2$ in order to eliminate the possible formation of the bimetallic Ru-ammine complexes previously discussed. This synthetic scheme is outlined below :

$$cis\text{-}Ru^{II}(bpy)_2Cl_2 \cdot 2H_2O \xrightarrow[N_2,\ acetone]{2\ Ag^+} cis\text{-}Ru^{II}(bpy)_2(acetone)_2^{2+} \longrightarrow$$

$$[Ru^{II}(NH_3)_4(bpyrm)](PF_6)_2 \longrightarrow [Ru^{II}(bpy)_2(bpyrm)Ru^{II}(NH_3)_4]^{4+}\ .$$

An analytically pure sample (PF_6^- salt) was obtained and it had the following elemental analysis (as trihydrate) :

Calc'd : C, 24.46; H, 2.93; N, 12.23.

Found : C, 24.58; H, 2.86; N, 12.06.

Based on these recent results, a new synthetic route for the trimetallic $[Ru^{II}(bpy)\{(bpyrm)Ru^{II}(NH_3)_4\}_2](PF_6)_6$ could be formulated. As in the previous example, $[Ru^{III}(NH_3)_4Cl_2]Cl$ could be replaced by $[Ru^{II}(NH_3)_4(bpyrm)](PF_6)_2$ in order to eliminate the side reactions associated with $[Ru^{II}(NH_3)_4(H_2O)_2]^{2+}$. Also, $[Ru^{II}(bpyrm)_2(bpy)](PF_6)_2$ could be replaced by $Ru^{III}(bpy)Cl_3(H_2O)$. The trimetallic species might then be formed in a manner analogous to the synthesis of $[Ru^{II}(bpyrm)_2(bpy)](PF_6)_2$ described in the experimental section.

Summary

The previous discussions have shown that both the bimetallic

$$[Ru^{II}(bpy)_2(bpyrm)Ru^{II}(NH_3)_4](PF_6)_4,$$

and trimetallic

$$[Ru^{II}(bpy)\{(bpyrm)Ru^{II}(NH_3)_4\}_2](PF_6)_6$$

species were synthesized. Despite the presence of an inseparable impurity, we did generate and measure the spectrophotometric properties (UV-vis-NIR) of both :

$$[Ru^{II}(bpy)_2(bpyrm)Ru^{III}(NH_3)_4]^{5+}$$

and

$$[Ru^{II}(bpy)\{(bpyrm)Ru^{III}(NH_3)_4\}_2]^{8+} .$$

Recent investigations[9] have produced a new synthetic technique that has yielded pure $[Ru^{II}(bpy)_2(bpyrm)Ru^{II}(NH_3)_4](PF_6)_4$. In light of this discovery, it is possible that a reworked synthesis of the trimetallic species could be found in order to characterize the properties of :

$$[(NH_3)_4Ru^{II}\text{-bpyrm-}Ru^{II}(bpy)\text{-bpyrm-}Ru^{III}(NH_3)_4]^{7+} .$$

If this [3,2,2] form of the trimetallic species is obtained in pure form and an "end-to-end" IVCT is observed, this complex would begin a series of interesting electron transfer model compounds.

Table 3-1 : Summary of Starting Materials UV-vis Data

Complex	Solvent	Observed nm (ϵ x 10^{-3} M^{-1} cm^{-1})	Literature nm (ϵ x 10^{-3} M^{-1} cm^{-1})	
cis-$Ru^{II}(bpy)_2Cl_2 \cdot 2H_2O$	CH_3CN	551.0 (8.64)	547.0 (8.91)	ref.1
		(sh) 486.0 (4.52)		
		377.0 (8.48)	376.0 (8.71)	
		297.0 (47.9)	298.0 (50.1)	
		(sh) 291.0 (37.6)		
		241.0 (20.8)	241.0 (21.4)	
$[Ru^{II}(bpy)_2(bpyrm)](PF_6)_2 \cdot H_2O$	CH_3CN	(sh) 472.0 (5.7)	(sh) 480.0	ref.2,3
		423.0 (9.7)	422.0 (9.7)	
		361.0 (6.4)	360.0 (6.4)	
		288.0 (47.4)	294.0 (48.0)	
		239.0 (36.4)	236.0 (40.0)	
$[Ru^{II}(bpyrm)_2(bpy)](PF_6)_2$	CH_3CN	(sh) 458.0 (6.05)	(sh) 460.0	ref.3
		420.0 (6.69)	420.0 (9.40)	
		369.0 (7.28)	368.0 (9.80)	
		330.0 (9.91)	326.0 (12.0)	
		283.5 (17.1)	283.0 (28.0)	
		258.0 (31.3)	255.0 (39.0)	

Table 3-1 : cont.

Complex	Solvent	Observed nm (ϵ x 10^{-3} M^{-1} cm^{-1})	Literature nm (ϵ x 10^{-3} M^{-1} cm^{-1})	
$[Ru^{III}(NH_3)_4Cl_2]Cl$	H_2O	342.5 (1.40)	350.0 (1.48)	ref.5
		301.0 (1.19)	308.0 (1.28)	
		251.0 (.430)	260.0 (.460)	

Table 3-2 : Summary of Cyclic Voltammetry Data for Starting Materials[a]

Complex	Observed	Literature	
cis-$Ru^{II}(bpy)_2Cl_2 \cdot 2H_2O$	0.326 (72)[b]	0.31	ref.1
$[Ru^{II}(bpy)_2(bpyrm)](PF_6)_2 \cdot H_2O$	1.372 (66)[c]	1.40	ref.2,3
$[Ru^{II}(bpyrm)_2(bpy)](PF_6)_2$	1.501 (66)[c]	1.55	ref.3,4
$[Ru^{III}(NH_3)_4Cl_2]Cl$	-0.11 (irreversible)[d]	-0.11	ref.5

[a]Platinum (for CH_3CN) or freshly polished glassy carbon (for aqueous solutions) working electrodes were used, along with a Pt auxiliary electrode, and a saturated sodium chloride calomel (SSCE) reference electrode. Potentials are in volts. Scan rate was 100 mV/s. Values in brackets indicate peak separations ($\Delta E_p = E_{anodic} - E_{cathodic}$) in mV. [b]0.1M TBAH/$CH_3CN$. [c]0.1M TEAP/$CH_3CN$. [d]0.1M KCl/$H_2O$.

Table 3-3 : UV-vis Data of $[Ru^{II}(bpy)_2(bpyrm)Ru^{II}(NH_3)_4](PF_6)_4$ in the [2,2] Oxidation State in CH_3CN.

Observed nm (ϵ x 10^{-3} M^{-1} cm^{-1})	Transition assignments
687.0 (3.1)	$d\pi$ [Ru^{II}-ammine] -› π^*[bpyrm] MLCT
498.0 (5.3)	$d\pi$ [Ru^{II}-bpy] -› π^*[bpyrm] MLCT
423.0 (13.2)	$d\pi$ [Ru^{II}-bpy] -› π^*[bpy] MLCT $d\pi$[Ru^{II}-ammine] -› π^*[bpyrm] MLCT
282.0 (31.6)	ligand π -› π^*[bpy & bpyrm]
254.0 (18.0)	ligand π -› π^*[bpy & bpyrm]
245.0 (18.0)	ligand π -› π^*[bpy & bpyrm]

Table 3-4 : UV-vis Data of $[Ru^{II}(bpy)\{(bpyrm)Ru^{II}(NH_3)_4\}_2](PF_6)_6$ in the [2,2,2] Oxidation State in CH_3CN.

Observed nm (ϵ x 10^{-3} M^{-1} cm^{-1})	Transition assignments
694.0 (7.2)	$d\pi$ [Ru^{II}-ammine] -› π^* [bpyrm] MLCT
435.0 (25.2)	$d\pi$ [Ru^{II}-bpy] -› π^* [bpyrm] MLCT $d\pi$[Ru^{II}-ammine] -› π^*[bpyrm] MLCT
(sh) 382.0	$d\pi$ [Ru^{II}-bpy]-› π^* [bpy] MLCT
272.0 (47.8)	ligand π -› π^*[bpy & bpyrm]
246.0 (37.2)	ligand π -› π^*[bpy & bpyrm]

Table 3-5 : Summary of Cyclic Voltammetry Data [a]

Complex	Solvent	$E_{1/2}$, V (ΔE_p, mV)
$[Ru^{II}(bpy)_2(bpyrm)Ru^{II}(NH_3)_4](PF_6)_4$	CH_3CN/0.1M TEAP	+0.899 (70) +1.626 (128)
$[Ru^{II}(bpy)\{(bpyrm)Ru^{II}(NH_3)_4\}_2](PF_6)_6$	CH_3CN/0.1M TEAP	+0.917 (100)
$[Ru^{II}(NH_3)_4(bpyrm)](PF_6)_2$	CH_3CN/0.1M TBAH	+0.660 (58)[b]

[a]Platinum (for CH_3CN) or freshly polished glassy carbon (for aqueous solutions) working electrodes were used, along with a Pt auxiliary electrode, and a saturated sodium chloride calomel (SSCE) reference electrode. Potentials are in volts. Scan rate was 100 mV/s. TEAP = tetraethylammonium perchlorate. TBAH = tetrabutylammonium hexafluorophosphate. Values in brackets indicate peak separations ($\Delta E_p = E_{anodic} - E_{cathodic}$) in mV. [b] Reference 9.

Table 3-6 : UV-vis Data of $[Ru^{II}(bpy)_2(bpyrm)Ru^{II}(NH_3)_4](PF_6)_4$ in the [2,2] and [2,3] Oxidation State in CH_3CN.

[2,2] Observed nm (ϵ x 10^{-3} M^{-1} cm^{-1})	[2,3] Observed nm (ϵ x 10^{-3} M^{-1} cm^{-1})	[2,3] Transition assignments
687.0 (3.1)		
498.0 (5.3)	581.0 (2.6)	$d\pi$ [Ru^{II}-bpy] -› π^*[bpyrm] MLCT
423.0 (13.2)	411.0 (10.6)	$d\pi$ [Ru^{II}-bpy] -› π^*[bpy] MLCT
282.0 (31.6)	279.0 (32.3)	ligand π -› π^*[bpy & bpyrm]
254.0 (18.0)		
245.0 (18.0)	247.0 (22.1)	ligand π -› π^*[bpy & bpyrm]

Table 3-7 : UV-vis Data of[Ru^{II}(bpy){(bpyrm)$Ru^{II}(NH_3)_4$}2]$(PF_6)_6$ in the [2,2,2] and [3,2,3] Oxidation State in CH_3CN.

[2,2,2] Observed nm (ϵ x 10^{-3} $M^{-1}cm^{-1}$)	[3,2,3] Observed nm (ϵ x 10^{-3} $M^{-1}cm^{-1}$)	[3,2,3] Transition assignments
694.0 (7.2)		
435.0 (25.2)	533.0 (6.4)	$d\pi$ [Ru^{II}-bpy] -› π^* [bpyrm] MLCT
(sh) 382.0	380.0 (16.1)	$d\pi$ [Ru^{II}-bpy]-› π^* [bpy] MLCT
272.0 (47.8)	265.0 (49.3)	ligand π -› π^*[bpy & bpyrm]
246.0 (37.2)	246.0 (40.0)	ligand π -› π^*[bpy & bpyrm]

Figure 3-1 : UV-vis Spectrum of cis-$Ru^{II}(bpy)_2Cl_2 \cdot 2H_2O$ in CH_3CN.

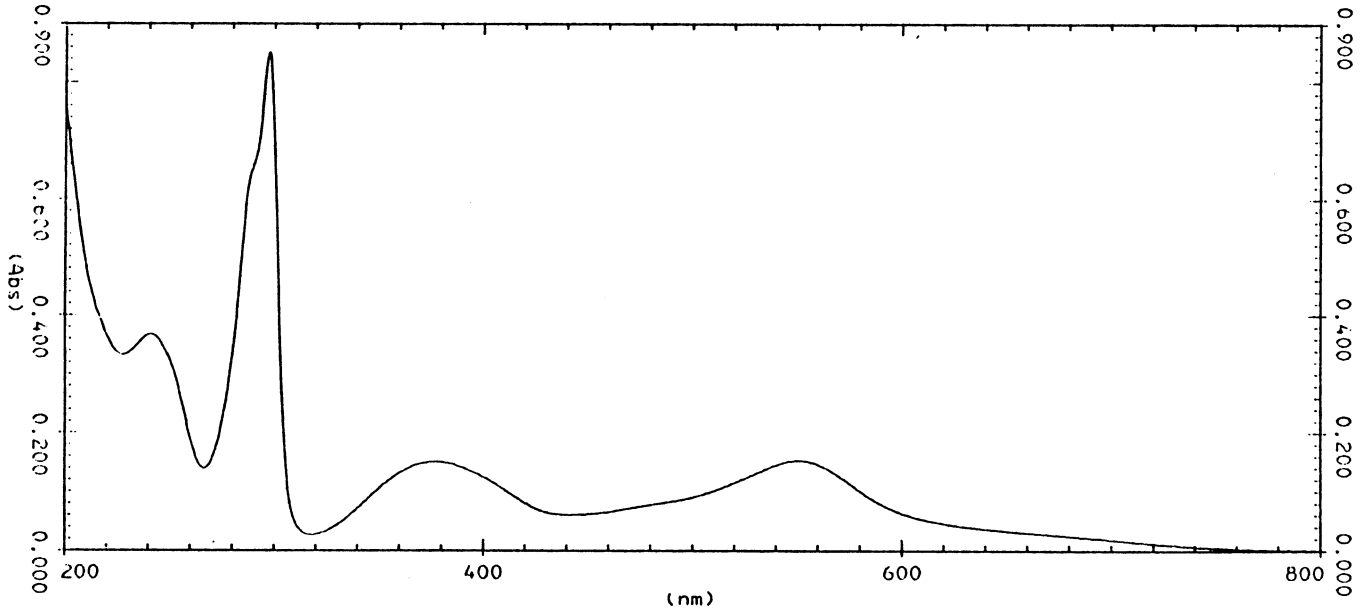

Figure 3-2 : Cyclic Voltammogram of cis-$Ru^{II}(bpy)_2Cl_2 \cdot 2H_2O$ in 0.1M TBAH/CH_3CN.

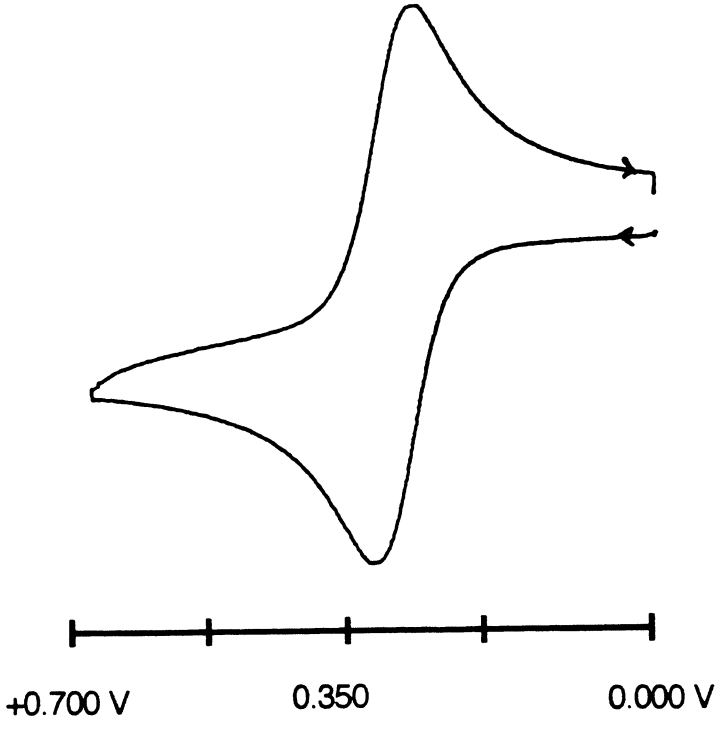

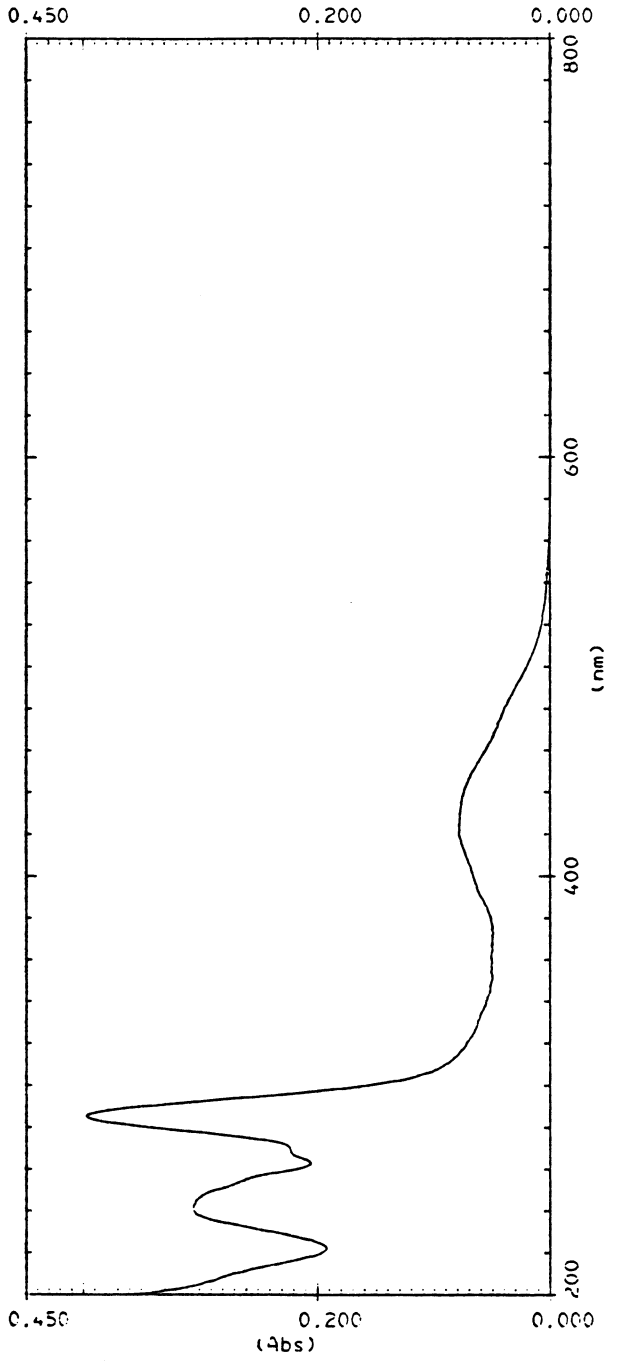

Figure 3-3 : UV-vis Spectrum of $[Ru^{II}(bpy)_2(bpyrm)](PF_6)_2 \cdot H_2O$ in CH_3CN.

Figure 3-4 : Cyclic Voltammogram of $[Ru^{II}(bpy)_2(bpyrm)](PF_6)_2 \cdot H_2O$ in 0.1M TBAH/CH_3CN.

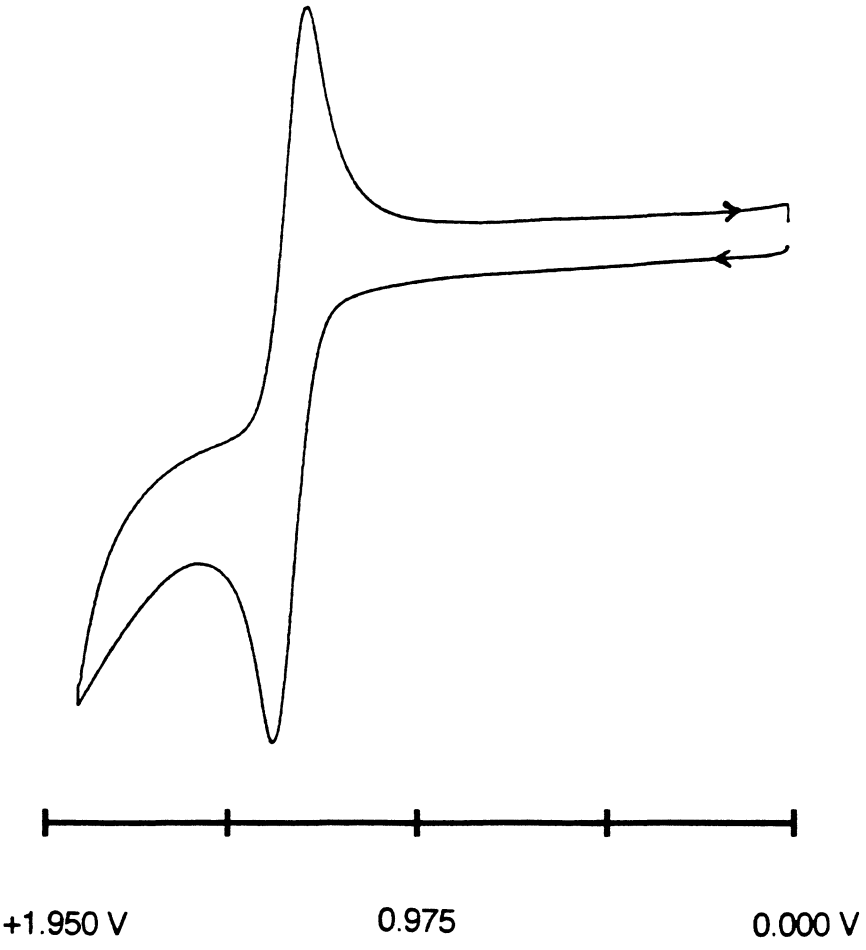

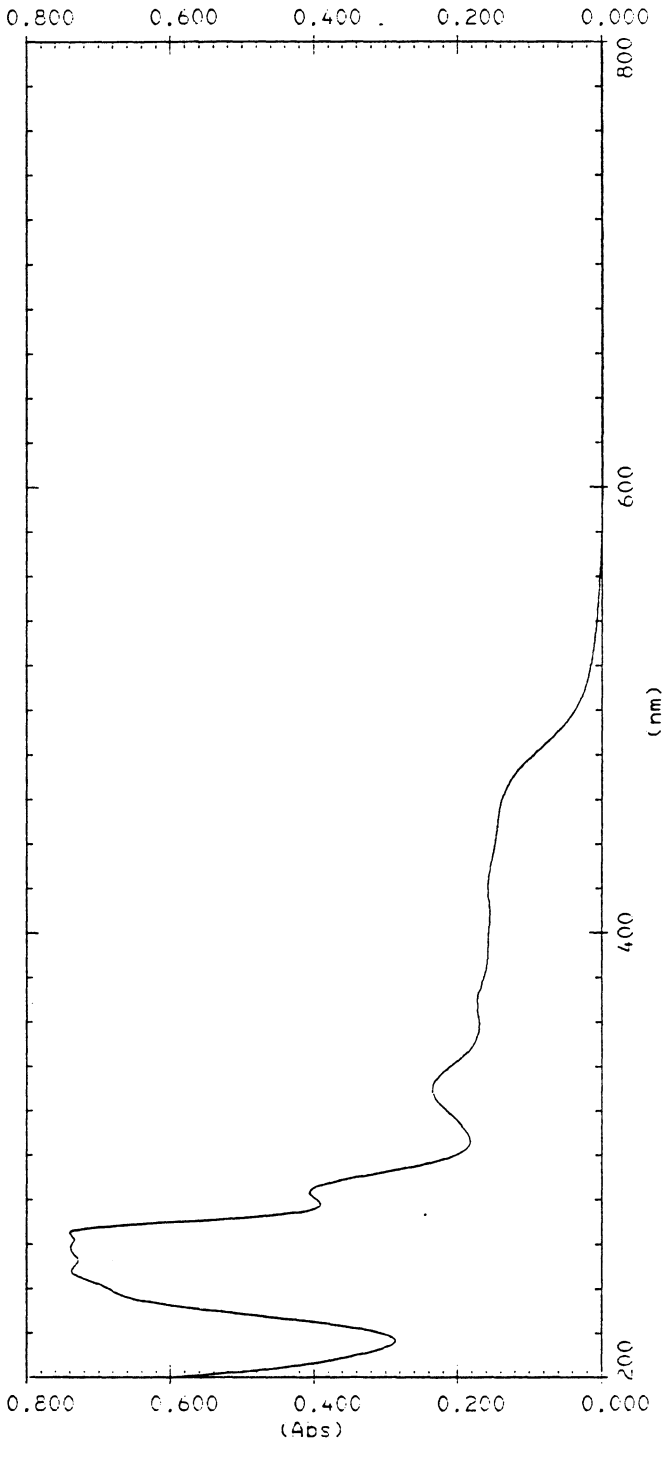

Figure 3-5 : UV-vis Spectrum of $[Ru^{II}(bpy)(bpyrm)_2](PF_6)_2$ in CH_3CN.

Figure 3-6 : Cyclic Voltammogram of $[Ru^{II}(bpy)(bpyrm)_2](PF_6)_2$ in 0.1M TEAP/CH_3CN.

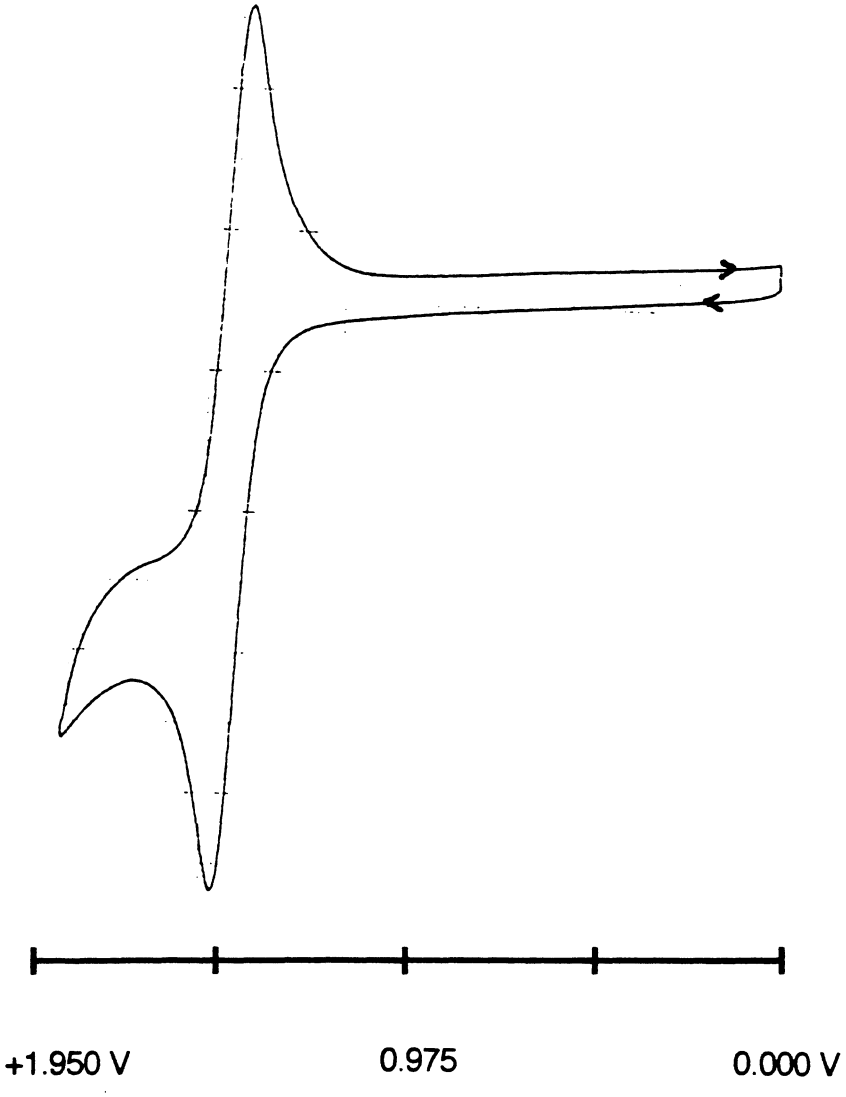

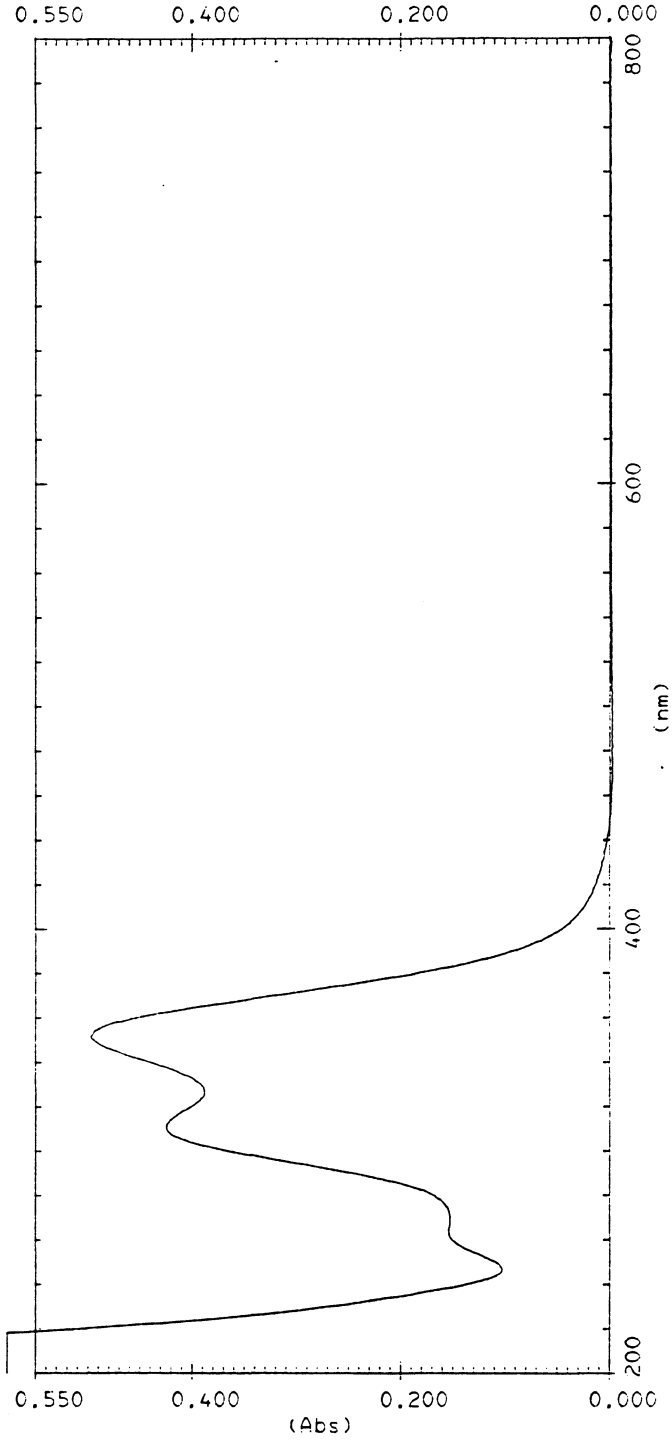

Figure 3-7 : UV-vis Spectrum of $[Ru^{III}(NH_3)_4Cl_2]Cl$ in aqueous solution.

Figure 3-8 : Cyclic Voltammogram of $[Ru^{III}(NH_3)_4Cl_2]Cl$ in 0.1M KCl/H_2O .

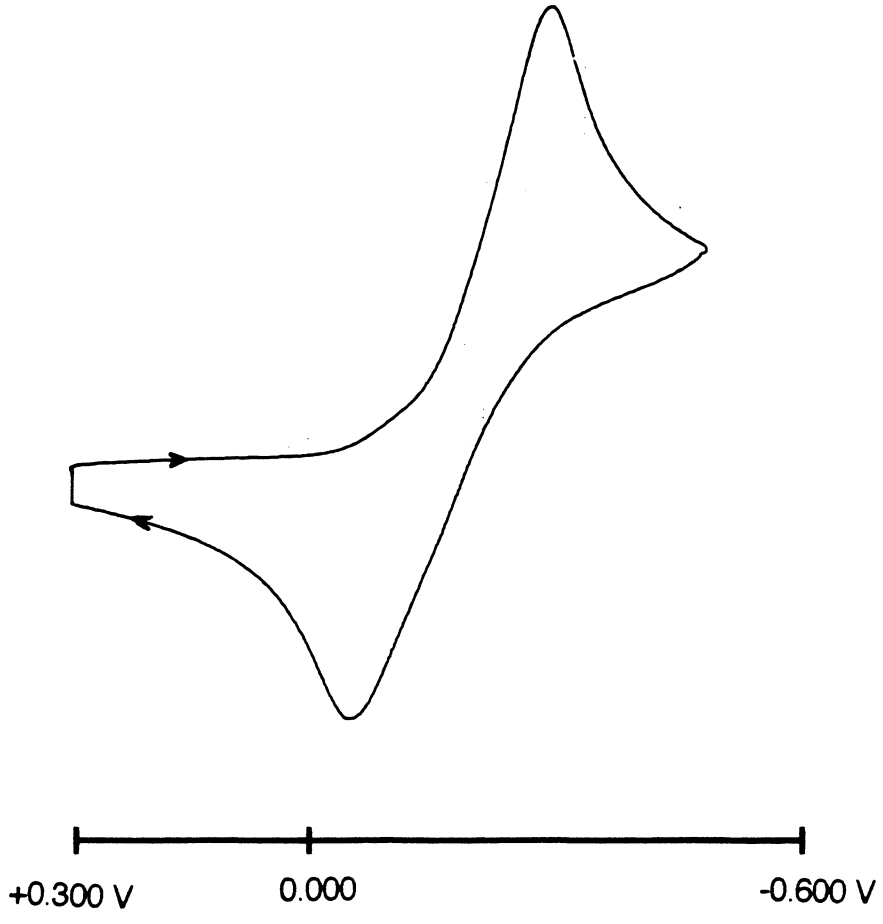

Figure 3-9 : UV-vis Spectrum of $[Ru^{II}(bpy)_2(bpyrm)Ru^{II}(NH_3)_4](PF_6)_4$ in the [2,2] Oxidation State in CH_3CN.

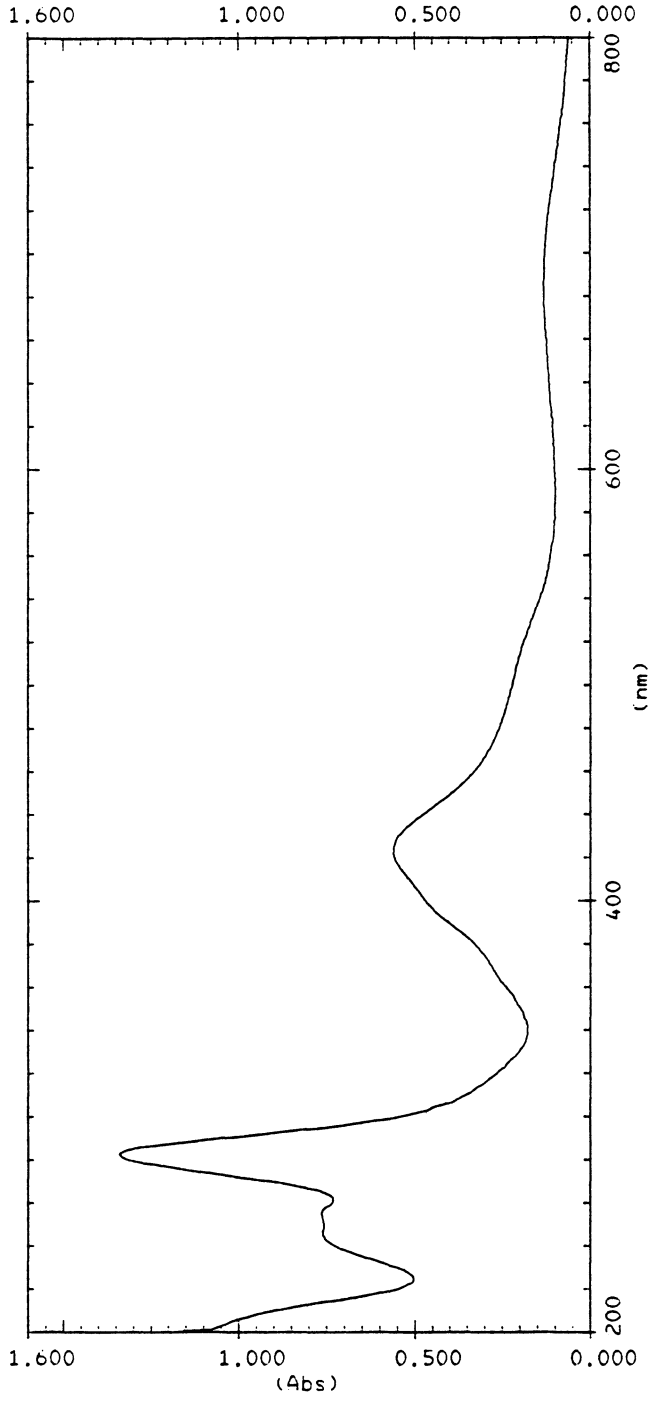

Figure 3-10 : Cyclic Voltammogram of $[Ru^{II}(bpy)_2(bpyrm)Ru^{II}(NH_3)_4](PF_6)_4$ in 0.1M TEAP/CH_3CN.

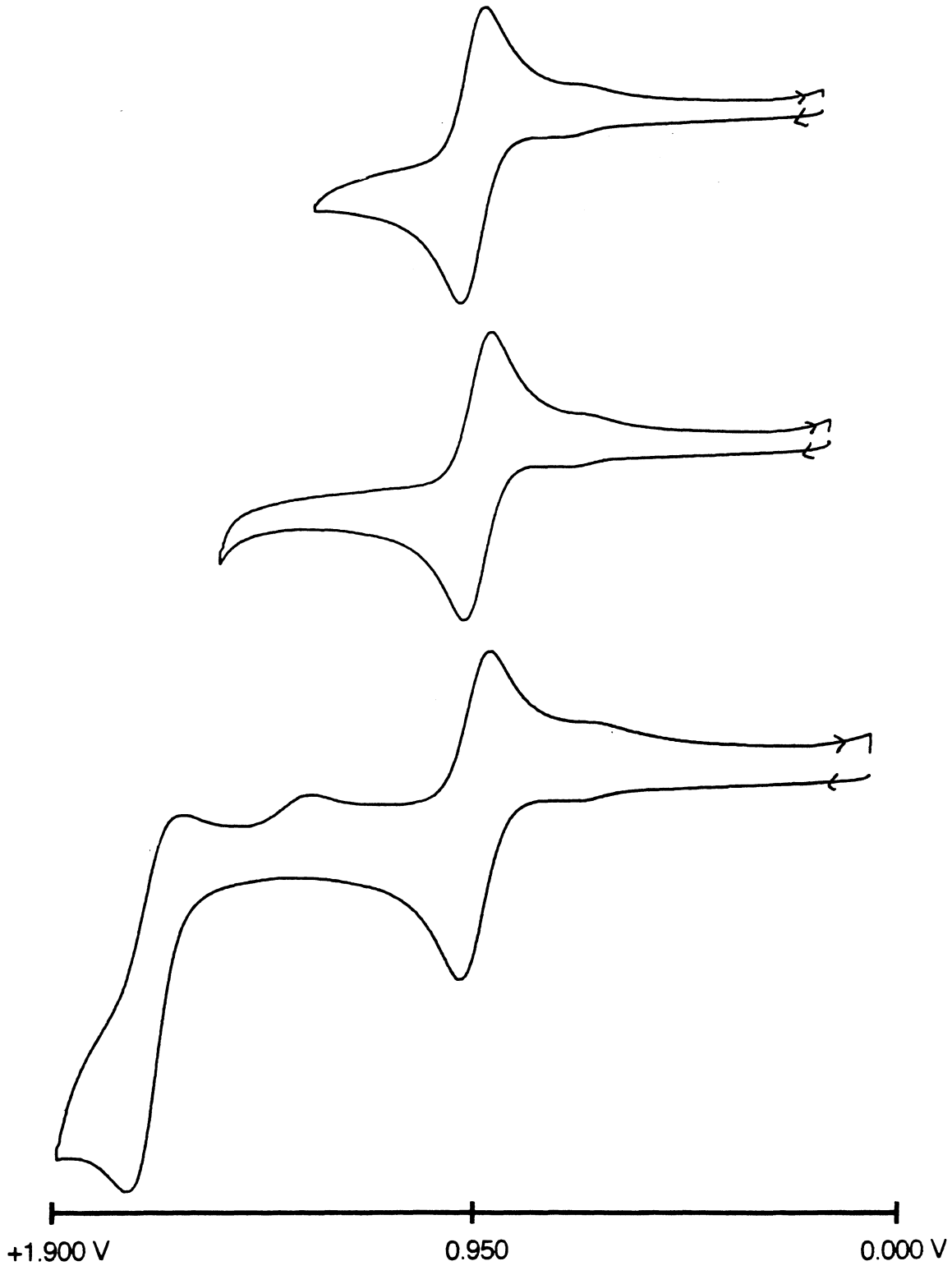

Figure 3-11 : UV-vis Spectrum of $[Ru^{II}(bpy)\{(bpyrm)Ru^{II}(NH_3)_4\}_2](PF_6)_6$ in the [2,2,2] Oxidation State in CH_3CN.

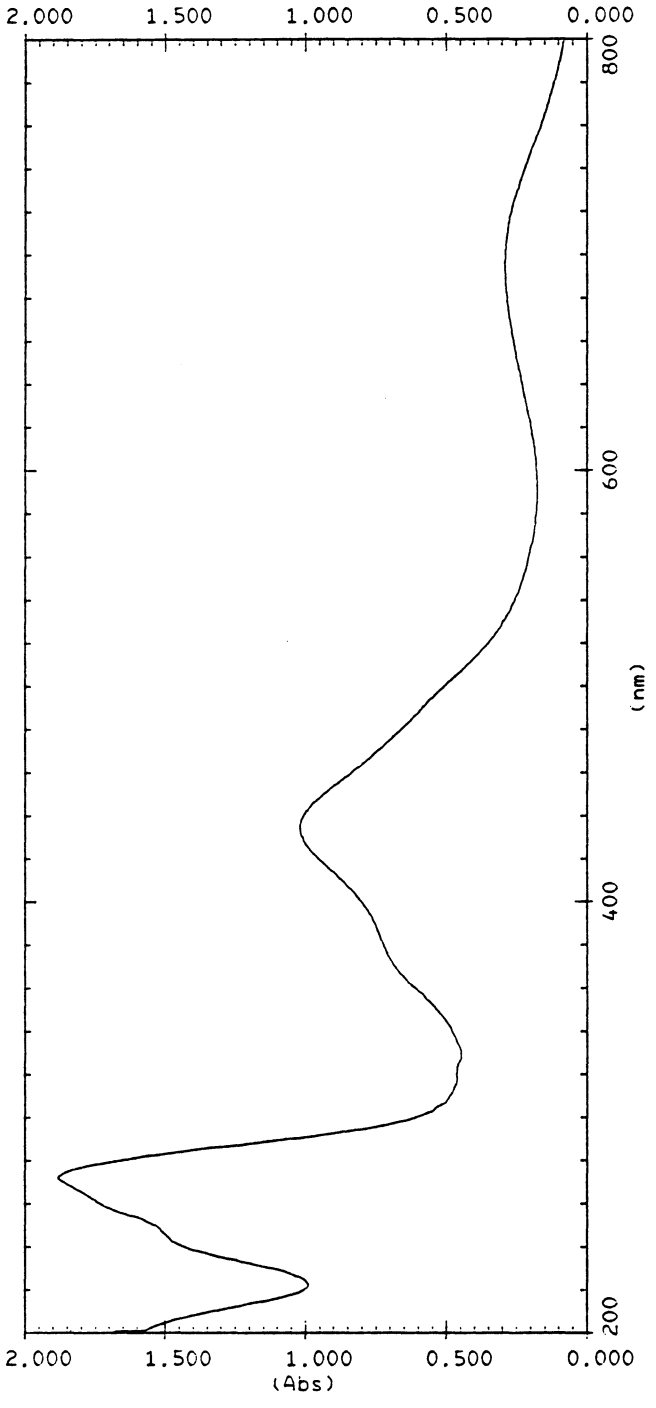

Figure 3-12 : Cyclic Voltammogram of $[Ru^{II}(bpy)\{(bpyrm)Ru^{II}(NH_3)_4\}_2](PF_6)_6$ in 0.1M TEAP/CH_3CN.

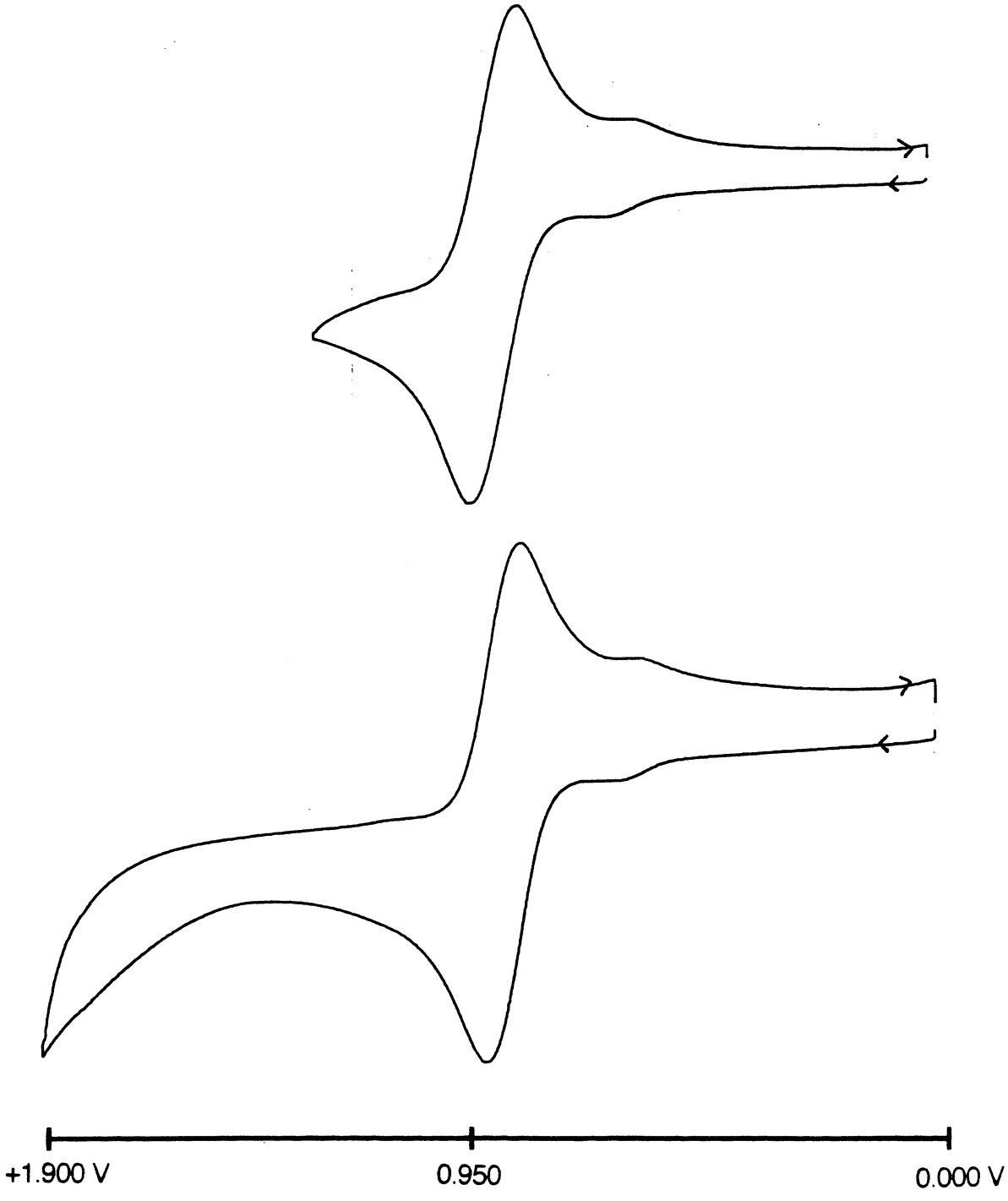

Figure 3-13 : UV-vis Spectrum of $[Ru^{II}(bpy)_2(bpyrm)Ru^{III}(NH_3)_4](PF_6)_4$ in the [2,3] Oxidation State in 0.1M TBAH/CH_3CN.

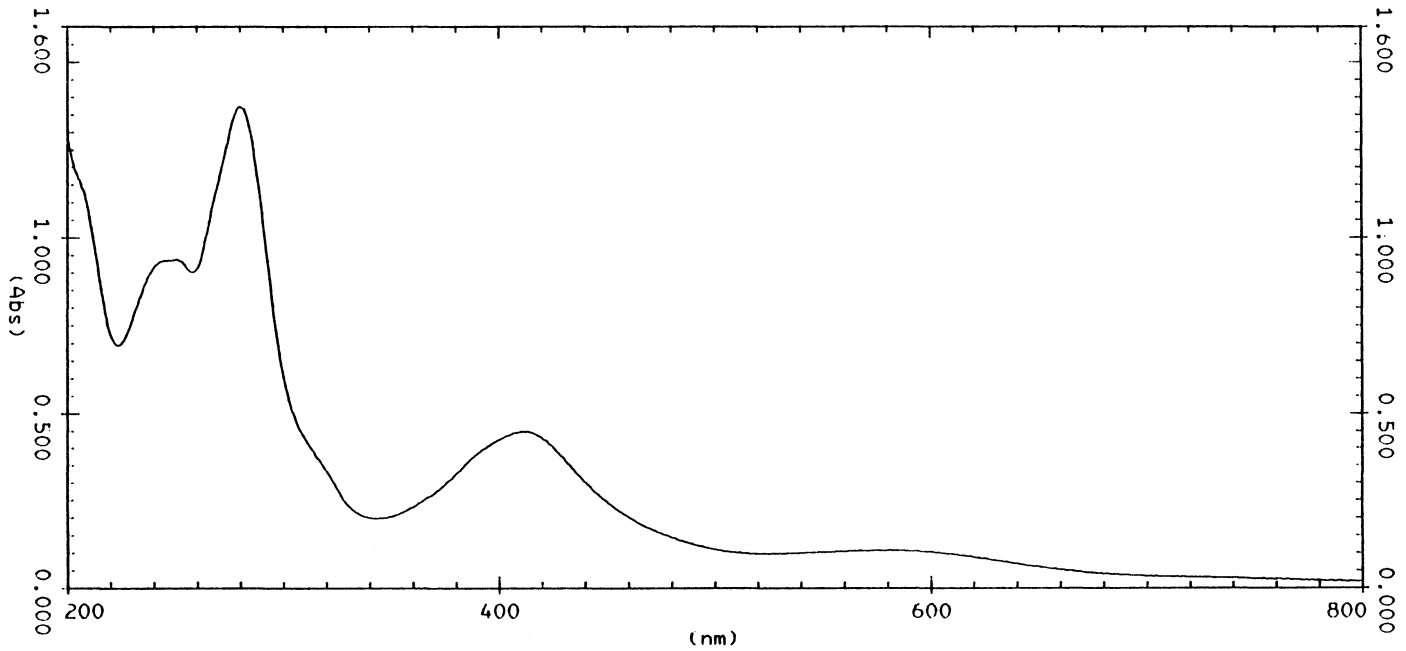

Figure 3-14 : UV-vis Spectrum of $[Ru^{II}(bpy)\{(bpyrm)Ru^{III}(NH_3)_4\}_2](PF_6)_6$ in the [3,2,3] Oxidation State in 0.1M TEAP/CH_3CN.

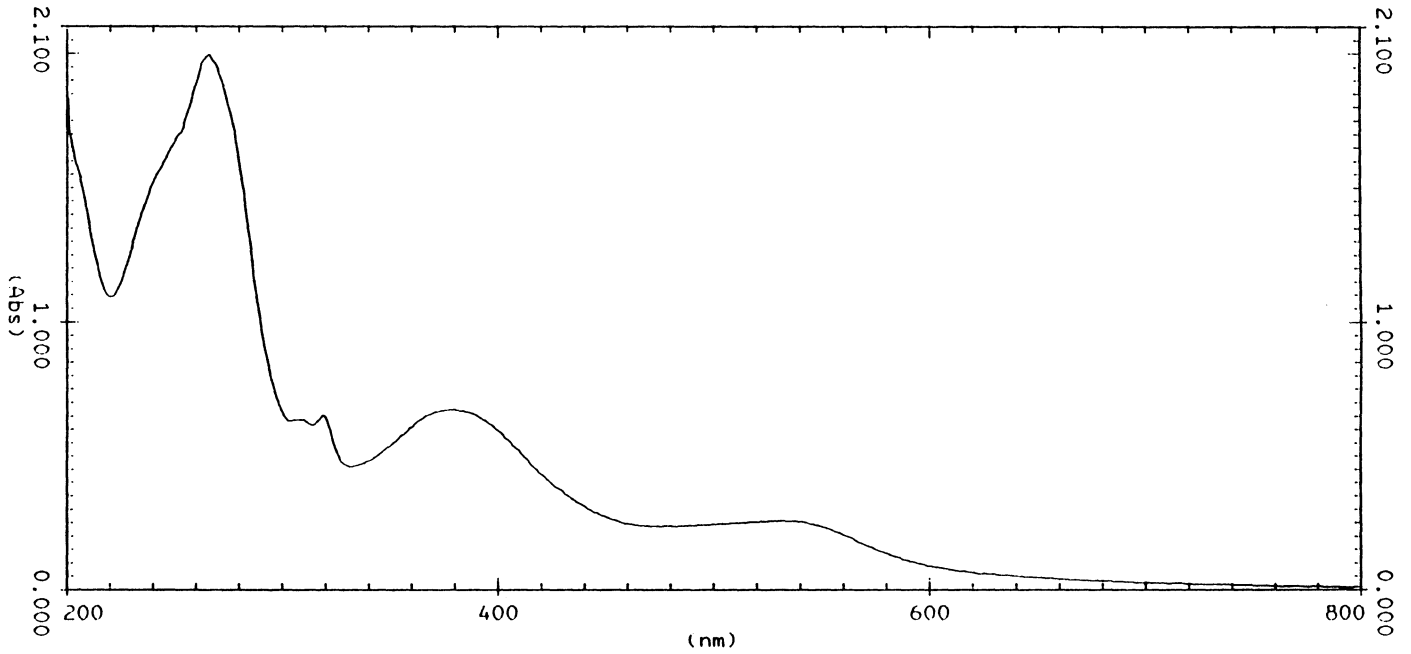

References

1. a.Crutchley, R. J.; Lever, A. B. *Inorg. Chem.* **1982**, *21*, 2276-2282.

   b.Sullivan, B. P.; Salmon, D. J.; Meyer, T. J. *Inorg. Chem.* **1978**, *17*, 3334-3341.

2. Mack, K. B.; Rillema, D. P. *Inorg. Chem.* **1982**, *21*, 3849-3854.

3. Conrad, D.; Allen, G.; Meyer, T. J.; Rillema, D. P. *Inorg. Chem.* **1983**, *22*, 1617-1622.

4. Small differences in $E_{1/2}$ values between this work and the literature are most likely the result of different electrochemical cell arrangements.

5. a.Pell, S. D.; Sherban, M. M.; Tramontano, V.; Clarke, M. J. *Inorganic Synthesis* ;Kaesz, H. D., Ed.; John Wiley & Sons: New York, 1989, Vol.26, pp.65-68.

   b.Chaisson, D. A.; Hintze, R. E.; Stuermer, D. H.; Petersen, J. D.; McDonald, D. P.; Ford, P. C. *J. Am. Chem. Soc.* **1972**, *94*, 6665-6673.

   c.Marchant, J. A.; Matsubara, T.; Ford, P. C. *Inorg. Chem.* **1977**, *16*, 2160-2165.

   d.Ford also conducted his electrochemistry in a more acidic environment (0.001 M HCl/0.199NaCl) whereas our electrochemistry was recorded in (0.1 M KCl/H_20).

   e.Matsubara, T; Ford, P. C. *Inorg. Chem.* **1978**, *17*, 1746.

6. Petersen, J. D.; Ruminski, R. R. *Inorg. Chem.* **1982**, *21*, 3706-3708.

7. Dose, E. V.; Wilson, L. J. *Inorg. Chem.* **1978**, *17*, 2660-2666.

8. Johnson, E. C.; Sullivan, B. P.; Salmon, D. J.; Adeyemi, S. A.; Meyer, T. J. *Inorg. Chem.* **1978**, *17*, 2211-2215.

9. Pavinato, R. A.; Walk, J. A.; McGuire, M. E. *Inorg. Chem.* **1993**, *32*, 4982-4984.

10. Callahan, R. W.; Brown, G. M.; Meyer, T. J. *Inorg. Chem.* **1975**, *14*, 1443-1453.

11. Sahai, R.; Morgan, L.; Rillema, D. P. *Inorg. Chem.* **1988**, *27*, 3495-3500.

12. Bignozzi, C. A.; Paradisi, S. R.; Scandola, F. *Inorg. Chem.* **1988**, *27*, 408-414.

Appendix I

Reagents/Conditions [a]	Method [b]	Purification [c]	Data [d]
Ru1 (.0714 g, .0812 mmol)		Alumina (AA)	UV : 3.81-88
in 1:4 acetone/abs.EtOH		in acetone	EC : 4.110-112
RuN4 (.0251 g, .0911 mmol) in water	A		
AgTFMS (.0704 g, .2739 mmol)		G-10 (AB)	
Reflux (1-39)		in 0.1M KCl	
		LH-20 (AC)	
		in 1:1 MeOH/acetone	
		LH-20 (AD)	
		in 1:1 MeOH/acetone	

---

[a] Ru1 = $[Ru^{II}(bpy)_2(bpyrm)](PF_6)_2$

RuN4 = $[Ru^{III}(NH_3)_4Cl_2]Cl$

AgTFMS = silver trifluoromethanesulfonate

[b] Refer to Method Description.

[c] Refer to Purification Description.

[d] UV = UV-VIS spectra

EC = Cyclic Voltammograms

Reagents/Conditions	Method	Purification	Data
Ru1 (.100 g, .114 mmol) in 1:1 EtOH/acetone	B	LH-20 (AE)	UV : 3.127-138
RuN4 (.0478 g, .173 mmol) in water		in 1:1 MeOH/acetone	3.142-160
AgTFMS (.134 g, .522 mmol), Reflux (1-49)			EC : 4.150
Ru1 (.0957 g, .109 mmol) in 8:1 EtOH/acetone	C	KPF_6 (AF)	UV : 3.161-169
RuN4 (.0335 g, .122 mmol) in water		in water	
gentle Reflux (1-51)			
Ru1 (.1800 g, .205 mmol) in acetone	D	Salt Switched (AG)	EC : 4.151-154
RuN4 (.0058 g, .0210 mmol) in water			4.166-171
Temp. 40°C, NH_4PF_6 in water, (2-8)			
Ru1 (.100 g, .114 mmol) in acetone	E	Salt Switched (AH)	UV : 3.182-185
RuN4 (.095 g, .345 mmol)			
Temp. 40°C, (2-11)		LH-20 in acetone (AI)	

Reagents/Conditions	Method	Purification	Data
Ru1 (.100 g, .114 mmol) in acetone RuN4 (.0353 g, .128 mmol) in water Temp. 30°C, (2-30)	F	Salt Switched (AJ)	EC : 4.181-182
Ru1 (.105 g, .119 mmol) in acetone RuN4 (.0416 g, .151 mmol) in water Temp. 40°C, (2-32)	G	NH_4PF_6 (AK) in water	

Method Description

A) RuN4 and Ru1 were added to separate flasks containing 10 mL of water and 50 mL of a 1:4 acetone/abs. EtOH solution, respectively. Both solvents had previously been deaerated for 30 minutes with argon. See Figure 2-1 for reaction set-up. While an inert atmosphere was maintained, Zn/Hg amalgam and AgTFMS were added to the flask containing RuN4. Immediately after adding the AgTFMS, a dark grey precipitate formed. The reactant was allowed to stir over the amalgam for 30 minutes. The RuN4 was then transferred via a stainless steel cannula thru a glass frit into the flask containing Ru1. The solution gradually turned from an orange-red to a dark red color. The solution was heated to reflux for 2.5 hours, and then cooled to room temperature and KPF_6 (.1008 g, .548 mmol) was added. The dark green solution was then rotovapped to dryness.

B) RuN4, Ru1, and AgTFMS were added to separate flasks containing 15 mL of water, 60 mL of a 1:5 acetone/abs. EtOH solution, and air, respectively. All solvents had previously been deaerated for 30 minutes with argon. While an inert atmosphere was maintained in all flasks, Zn/Hg amalgam was added to the flask containing RuN4 and stirred for 30 minutes. The RuN4 was then transferred via a cannula to a flask containing AgTFMS, and stirred for 45 minutes. The silver-grey solid that was formed was allowed to settle, and the solution was then transferred via a cannula thru a glass frit to a flask containing the Ru1. The mixture was heated to reflux for 5 hours. The reaction mixture was then transferred via a cannula to a flask containing a fresh Zn/Hg

amalgam and stirred for 1hour. When the solution was transferred back from the amalgam to the reaction vessel, a green precipitate was collected off of the amalgam with EtOH. The solution was heated to reflux and allowed to stir for 18 hours and became very dark almost black in color. The solution was cooled to room temperature, KPF_6 (.128 g, .696 mmol) was added, and then rotovapped to dryness leaving a black solid.

C) RuN4 and Ru1 were added to separate flasks containing 12 mL of water and 40 mL of a 8:1 abs.EtOH/acetone solution respectively. Both solvents had previously been deaerated for 30 minutes with argon. See Figure 2-1 for reaction setup. While an inert atmosphere was maintained Zn/Hg amalgam was added to the flask containing RuN4, and stirred for 30 minutes. The RuN4 was then transferred via a cannula into the reaction vessel containing the Ru1. The solution immediately turned a very dark color. The mixture was heated to a gentle reflux for 7.5 hours. The solution was cooled to room temperature, KPF_6 (.1214 g, .660 mmol) was added, and then rotovapped to dryness.

D) RuN4 and Ru1 were added to separate flasks containing 20 mL of water and 50 mL of acetone respectively. Both solvents had previously been deaerated for 20 minutes with argon. See Figure 2-1 for setup. While an inert atmosphere was maintained, Zn/Hg amalgam was added to the flask containing RuN4. The reactant was allowed to stir over the amalgam for 30 minutes, and the color had changed from an orange-yellow to a golden yellow. At the same time as the amalgam was

added, the flask containing Ru1 was heated to 40°C. The RuN4 was then transferred over via a cannula into the reaction vessel containing Ru1. The solution immediately turned from an orange-red color to black. The solution was heated at 40°C for 8 hours. The reaction mixture was cooled to room temperature and rotovapped until only ~10 mL of water remained. A saturated solution of NH_4PF_6 was added dropwise until a dark green precipitate formed. The product was collected on a glass frit and dried in vacuo.

E) The procedure was followed as described in D except for: Ru1 was dissolved in 40 mL of acetone; a three-fold excess of RuN4 was used; the reaction was heated to 40°C for 2.5 hours; and the precipitated product was washed with a few drops of ice cold water.

F) The procedure was followed as described in D except for: RuN4 was dissolved in 15 mL of water; and the reaction mixture was heated to 30°C for 45 minutes.

G) The procedure was followed as described in F except the reaction mixture was heated to 40°C for 4 hours.

Purification Description

AA) The crude compound from Method A (50 mg) was redissolved in a minimum amount of acetone and purified by column chromatography. The sample was chromatographed on a column of alumina (1.1 cm x 8 inches) previously developed with acetone. The flow rate was fast. The column was loaded and a dark main band stuck to the upper two inches of the column. The first band was eluted off with a 40/60 CH_3CN/acetone solution and was yellow in color. The second band was eluted off with CH_3CN and was light green in color. The main band was eluted off with a 50/50 EtOH/CH_3CN solution, evaporated to dryness, and stored in vacuo.

AB) The crude compound from Method A (30 mg) was redissolved in a minimum amount of 0.1M KCl and purified by column chromatography. The sample was chromatographed on a column of G-10 (1.1 cm x 20 inches) previously developed with .1M KCl. The column was loaded and two separate bands were formed. The main product was eluted (as a dark band), followed by a yellow impurity band. The main product was reduced in volume, upon which a cyclic voltammogram was taken.

AC) The crude compound from Method A (45 mg) was redissolved in a minimum amount of a 50/50 MeOH/acetone solution. The sample was chromatographed on a LH-20 column (1.1 cm x 13.5 inches) previously developed with a 50/50 MeOH/acetone solution. A very slow drop rate was used. The sample was loaded onto the column and the main band

was eluted followed by a yellow-brown band. The fractions were collected, evaporated, and stored in vacuo.

AD) The rest of the crude product from Method A and fraction #2 and #3 from AC were treated as described in AC except the column length was 1.1 cm x 23.5 inches.

AE) The crude compound was redissolved in a minimum amount of a 50/50 MeOH/acetone solution. The sample was chromatographed on a LH-20 column (2.7 cm x 14 inches) previously developed with a 50/50 MeOH/acetone solution. The column was loaded and the main band was eluted at a drop rate of 1 drop every 9 seconds. A "main band" was eluted but the entire column was left stained.

AF) The crude compound was redissolved in a minimum amount of water. The product was precipitated out by the dropwise addition of a saturated solution of KPF_6 while being cooled in an ice bath. The precipitate was collected on a fine glass frit and dried in vacuo.

AG) The crude product was redissolved in a minimum amount of acetone and filtered with very little solid collected. The filtrate was dripped into swirling ether to precipitate the green product. The precipitate was then collected on a fine glass frit, washed with ether and dried in vacuo. The compound was then dissolved in a minimum amount of acetone and a saturated solution (70/30 MeOH/acetone) of TEAC was added dropwise until almost all of the product had precipitated. The light green precipitate was collected on a fine glass frit (filtrate should be slightly

yellow or it hasn't worked) and dried in vacuo. The chloride salt of the compound was then redissolved in a minimum amount of water and a saturated solution of NH_4PF_6 was added dropwise until the green precipitate formed. The precipitate was collected, and washed with ether. The product was then dried in vacuo. The dried product was then redissolved in a minimum amount of acetone and dripped into ~80 mL of swirling ether. The green precipitate was collected on a fine glass frit, washed with ether, and dried in vacuo. This process of "salt-switching" was then repeated two more times.

AH) The crude product was treated as described in AG.

AI) The product (that was collected in AH) was redissolved in a minimum amount of acetone and purified by column chromatography. The sample was chromatographed on a column of LH-20 (1.1 cm x 4.5 inches) previously developed with acetone. The column was loaded and a dark green band stuck to the top. The main cut (dark green) was eluted, followed by an orange-brown band. The main band was evaporated to dryness and stored in vacuo.

AJ) The crude product was treated as described in AG.

AK) The crude product was treated as described in AG.

Appendix II

Reagents/Conditions [a]	Method [b]	Purification [c]	Data [d]
Ru (.100 g, .116 mmol)	A	LH - 20 (AA)	UV : 3.11-13
RuN5 (.1463 g, .231 mmol)		in EtOH	3.14a, 15a
Solvent = abs. EtOH, Rm. Temp. (1-16)			EC : 4. 40-45
Ru (.102 g, .118 mmol) in 10 ml acetone	B	LH - 20 (AB)	UV : 3.14-17
RuN5 (.1489 g, .235 mmol) in 10 ml Abs. EtOH		2:1 EtOH/acetone	EC : 4.48-50
Rm. Temp. (1-17)			
		Acetone dripped	EC : 4.51-59
		cold ether (AC)	
		G-10 water (AD)	EC : 4.60-64
		G-10 0.1M KCl (AE)	EC : 4.65

[a] Ru = $[Ru^{II}(bpy)(bpyrm)_2](PF_6)_2$
RuN5 = $[Ru^{II}(NH_3)_5(TFMS)](TFMS)_2$

[b] Refer to Method Description.

[c] Refer to Purification Description.

[d] UV = UV-VIS spectra
EC = Cyclic Voltammograms

Reagents/Conditions	Method	Purification	Data
Ru (.102 g, .118 mmol)	C	KPF_6 (AF)	UV : 3.28-30
RuN5 (.1509 g, .238 mmol)		into ether	EC : 4.68
Solvent = acetone, refluxed for 1 hour			
Rm. Temp. for 4 hours (1-22)		CH_3CN into ether (AG)	EC : 4.78-80
		Sp-C25-120 in water (AH)	
		Fluorosil in acetone (AI)	
Ru (.102 g, .118 mmol) in 30 ml Abs. EtOH	D	LH-20 (AJ)	UV : 3.35-37, 46
RuN5 (.1534 g, .242 mmol) in 30 ml acetone		50/50 EtOH/acetone	EC : 4.81-87
Temp. 35°C (1-28)			
Ru (.050 g, .058 mmol)	E	LH-20 (AK)	UV : 3.55
RuN5 (.0742 g, .117 mmol)		50/50 MeOH/acetone	
Solvent = MeOH, Refluxed (1-30)			

Reagents/Conditions [e]	Method	Purification	Data
Ru (.100 g, .116 mmol) in acetone/MeOH	F	KPF_6 in water (AL)	UV : 3.71-80
RuN4 (.0655 g, .238 mmol) in water		-2°C overnight	
Refluxed (1-37)			
		Sephadex G-15 (AM)	EC : 4.101-109
		in water	
		Sephadex G-15 (AN)	EC : 4.109a-113
		0.1M KCl	
Ru (.1653 g, .192 mmol) in acetone/EtOH	G	KPF_6 in water (AO)	UV : 3.170-181
RuN4 (.211 g, .768 mmol) in water			EC : 4.155-157
Near Reflux (1-53)			4.162-165
Ru (.150 g, .174 mmol) in acetone	H	Salt switched (AP)	EC : 4.172
RuN4 (.143 g, .521 mmol) in water, Temp. 40°C (2-5)		three times	

[e] RuN4 = $[Ru(NH_3)_4Cl_2]Cl$

Method Description

A) Reactants were added to 20 mL of ethanol that had previously been deaerated for 30 minutes with argon. While an inert atmosphere was maintained Zn/Hg amalgam was added to the reaction vessel. Immediately a large amount of solid was noticed. After 25 minutes 10 mL of acetone was added. The solution changed from a red-orange color to black. The reaction was allowed to proceed for 80 minutes.

B) Reactants were combined, stirred, and deaerated for 20 minutes with argon. While an inert atmosphere was maintained, Zn/Hg amalgam was added to the reaction vessel. The reaction was allowed to proceed for 1.5 hours. The solution was dark blue in color.

C) Reactants were combined, stirred, and deaerated for 30 minutes with argon. While an inert atmosphere was maintained Zn/Hg amalgam (amalgam was washed with deaerated acetone upon which a grey layer appeared on the surface of the amalgam) was added to the reaction vessel and refluxed for 1 hour. Reaction was allowed to continue for 4 hours without heat. In an effort to keep fresh amalgam exposed to the reaction mixture, argon was bubbled thru the amalgam. The solution changed from a yellow-orange color to dark green.

D) RuN5 and Ru were added to separate flasks containing 30 mL of Abs. EtOH and 30 mL of acetone respectively. Both solvents had previously been deaerated for 30 minutes with argon. See Figure 2-1 for reaction setup. While an inert atmosphere was maintained, Zn/Hg amalgam was

added to the flask containing RuN5. The reactant was allowed to stir over the amalgam for 30 minutes, and the color changed from pale yellow to lime-green. The RuN5 was then transferred via a stainless steel cannula into the flask containing Ru. The solution immediately turned from an orange-red to a dark red color, and 60 mL of deaerated acetone was then added to the flask. The solution was heated to 35°C for 90 minutes, and then cooled to room temperature and allowed to stir for 2.5 hours. The solution was then reduced in volume to ~15 mL.

E) RuN5 was added to 50 mL of MeOH that had been deaerated for 30 minutes with argon. While an inert atmosphere was maintained Zn/Hg amalgam was added to the reaction vessel (MeOH did not react with the surface of the amalgam). After 30 minutes, Ru was added and the reaction mixture was stirred and heated to reflux. After 15 minutes, the reaction mixture had changed from a deep red color to black. The reaction was allowed to continue under reflux for 5 hours. The solution was cooled to room temperature and reduced in volume to ~5 mL.

F) RuN4 and Ru were added to separate flasks containing 7 mL of water and 5 mL of acetone respectively. Both solvents had previously been deaerated for 30 minutes with argon. See Figure 2-1 for reaction setup. While an inert atmosphere was maintained Zn/Hg amalgam was added to the flask containing RuN4, and stirred for 50 minutes. The RuN4 was then transferred via a cannula into the reaction vessel containing the Ru. The solution turned an ugly black color. The mixture was heated to reflux and after 30 minutes KPF_6 (.107 g, .58 mmol) was added.

Refluxing was continued for 3.5 hours, after which more KPF_6 (.107 g) was added to the reaction mixture. Refluxing was continued for 3 more hours, upon which the solution was then cooled to room temperature. The solution was then filtered thru a medium glass frit (no precipitate was collected) and then rotovapped to dryness. The resulting solid was not soluble in CH_3CN, but slightly soluble in acetone.

G) RuN4 and Ru were added to separate flasks containing 20 mL of water and 10 mL of acetone respectively. Both solvents had previously been deaerated for 30 minutes with argon. See Figure 2-1 for setup. While an inert atmosphere was maintained, Zn/Hg amalgam was added to the flask containing RuN4. The reactant was allowed to stir over the amalgam for 35 minutes, and the color had changed from an orange-yellow to a golden yellow. At the same time as the amalgam was added, 50 mL of deaerated abs. EtOH was added to the flask containing the Ru and the solution was heated to near reflux. The RuN4 was then transferred over via a cannula into the reaction vessel containing the Ru. The solution immediately turned from an orange-red color to black. The solution was heated to near reflux for 8 hours, then KPF_6 (.2119 g, 1.15 mmol) was added. The reaction mixture was cooled to room temperature and rotovapped to dryness and dried in vacuo.

H) The procedure was identical to G except for: Ru was dissolved in 50 mL of acetone; the reaction was heated to 40°C for 8 hours; and the mixture was rotovapped until only ~10 mL of water remained.

Purification Description

AA) The reaction mixture was purified by column chromatography. The mixture (~25 mL) was chromatographed on a LH-20 column (27 mm x 23 cm) previously developed with EtOH. The flow rate was fast. The sample was loaded onto the column and a red-brown precipitate stuck to the top. The main product was eluted as a dark green band, followed by a yellow-orange impurity band. The main band was reduced to 10 mL and then added dropwise into swirling ether to precipitate the compound. The product was collected on a fine glass frit, washed with a small amount of water causing most of the precipitate to dissolve. The product that was left was dried in vacuo.

AB) The reaction mixture (~20 mL) was chromatographed on a LH-20 column (34 mm x 28 cm) previously developed with a 2:1 EtOH/acetone solution. The flow rate was fast. The sample was loaded onto the column and eluted in a similar manner as AA. However, a dark grey band preceded the main band off of the column. The main band was reduced to10 mL, whereupon solid KPF_6 (.039 g, .212 mmol) was added. The solution was added dropwise into swirling ether to precipitate green product. The precipitate was collected on a fine glass frit and dried in vacuo.

AC) The crude compound from AB was added to 25 mL of swirling ether, and ~50 mL of acetone was added until all the solid was redissolved. The solution was cooled to -2 °C for 2 hours. Since no solid had formed, 50 mL of ether was added and cooling continued for 1 more

hour. The dark green precipitate was isolated by use of a fine glass frit, the yellow-orange filtrate was discarded and the product dried in vacuo.

AD) The crude compound from Method B (40 mg) was redissolved in a minimum amount of water and purified by column chromatography. The sample was chromatographed on a column of G-10 (1.1 cm x 12 inches) previously developed with water. The column was loaded and a dark precipitate (most of the sample) stuck to the top. Three distinct bands were collected. The first band eluted very fast and was light green in color. The second band was dark green in color and eluted at a moderate rate while the third orange band eluted very slowly. After the bands were collected the solvent was switched to 0.1M KCl and the remainder of the sample was collected.

AE) The crude compound from Method B was redissolved in a minimum amount of 0.1M KCl and purified by column chromatography. The sample was chromatographed on a column of G-10 (1.1 cm x 11 inches) previously developed with 0.1M KCl. The column was loaded and a orange-brown precipitate (eventually dissolved) stuck to the top. The main product was eluted (as a dark green band), followed by an orange-yellow impurity band. The main product was reduced in volume upon which a cyclic voltammogram was taken.

AF) KPF_6 (.0684 g, .371 mmol) was added to the reaction mixture. The dark green solution was reduced to ~7 mL and then added dropwise into swirling ether to precipitate the compound. The product was collected on a fine glass frit and dried in vacuo.

AG) The crude compound from AF was slowly redissolved in a minimum amount of CH_3CN. The solution was added dropwise into swirling ether that was cooled in a ice bath. The muddy, dark green product was collected on a fine glass frit and dried in vacuo.

AH) The crude compound from AF (50 mg) was redissolved in 1 mL of water and filtered. The filtrate was chromatographed on a Sephadex Sp-C25-120 column (1.1 cm x 12 inches) previously developed with water. The sample was loaded onto the column where it proceeded to stick to the top. An orange-brown band started to elute when the solvent was changed to 0.2M HCl. A red band started to elute when the concentration was increased to 0.3M. The main band remained stationary as the solvent concentration was gradually increased to 0.7M HCl. The main band remained near the top of the column and was removed along with the Sephadex it was bound to. Fractions were collected and reduced to ~2 mL.

AI) The remaining compound from AF was redissolved in a minimum quantity of acetone and chromatographed on a Fluorosil column (1.0 cm x 7 inches) previously developed with acetone. The sample was loaded on the column where a dark green band formed and proceeded to stick to the top. The solvent was switched to 5% MeOH/acetone and increased gradually to 100% MeOH. However the green band did not elute. The solvent was then switched to 10% H_2O/MeOH and increased gradually to 100% water, while the band continued to stick to the top. The main band later eluted with a weak solution of HCl.

AJ) The reaction mixture was purified by column chromatography. The mixture (~15 mL) was chromatographed on a LH-20 column (27 mm x 9 inches) previously developed with a 1:1 EtOH/acetone solution. The sample was loaded onto the column and eluted as described in AA. The main product was then treated as described in AB.

AK) The reaction mixture (~5 mL) was chromatographed on a LH-20 column (27 mm x 3 inches) previously developed with a 50/50 MeOH/acetone solution. The sample was loaded onto the column and the main band eluted followed by a brown band that stained the entire column. The main band was reduced to ~5 mL, whereupon KPF_6 (4 drops of a saturated solution) was added. The solution was dripped into ether to precipitate the black product. The precipitate was collected on a fine glass frit and dried in vacuo.

AL) The crude compound was redissolved in a minimum amount of water that was heated to 35°C, and KPF_6 (.2354 g, 1.28 mmol) was then added. The solution was cooled to -2°C overnight, and the green precipitate that formed was collected on a fine glass frit and dried in vacuo.

AM) The crude compound from AL (55 mg) was redissolved in 3 mL of water and was filtered thru a medium glass frit to remove insoluble matter. The solution was then purified by column chromatography. The sample was chromatographed on a column of G-15 (1.1 cm x 50 cm) previously developed with water. The column was loaded and initially the majority

of sample eluted very slowly. Two separate bands formed and were collected and rotovapped to dryness. The column was cleaned with a 0.1M KCl solution.

AN) The crude compound from AL (50 mg) was redissolved into 3 mL of 0.1M KCl and purified by column chromatography. The sample was chromatographed on a column of G-15 (1.1 cm x 20 inches) previously developed with 0.1M KCl. The column was loaded and a brown precipitate stuck to the top. The main product (dark green band) was eluted, followed by a yellow-green impurity band. KPF_6 (.243 g, 1.32 mmol) added to the main band and the precipitate that formed was collected on a fine glass frit and dried in vacuo.

AO) The crude compound was slowly redissolved in ~25 mL of water. The product was precipitated out by the dropwise addition of a saturated solution of KPF_6. The precipitate was collected on a fine glass frit and dried in vacuo. It was noticed that the filtrate was still very dark in color.

AP) The reaction mixture ~10 mL was cooled in an ice bath and the product was precipitated out in a manner described in AO. The crude product was then dissolved in a minimum amount of acetone and filtered. The filtrate was dripped into swirling ether to precipitate the green product. The precipitate was then collected on a fine glass frit, washed with ether, and dried in vacuo. The compound was then dissolved in a minimum amount of acetone and a saturated solution (70/30 MeOH/acetone) of TEAC was added dropwise until almost all of the product had precipitated. The light green precipitate was collected on

a fine glass frit and dried in vacuo. The chloride salt of the compound was then redissolved in a minimum amount of water and a saturated solution of NH_4PF_6 was added dropwise until the green precipitate formed. The precipitate was collected, and washed with EtOH and ether. The product was then dried in vacuo. The dried product was then dissolved in a minimum amount of acetone and dripped into ~80 mL of swirling ether. The green precipitate was collected on a fine glass frit, washed with ether, and dried in vacuo. This process of "salt-switching" was then repeated twice more.